



# The Plenus Cold Event Record in the Abyssal DSDP Site 367 (Cape Verde, Central Atlantic): Environmental Perturbations and Impacts on the Nitrogen Cycle

Laurent Riquier<sup>1\*</sup>, Pierre Cadeau<sup>2,3</sup>, Julien Danzelle<sup>1</sup>, François Baudin<sup>1</sup>, Emmanuelle Pucéat<sup>2</sup> and Christophe Thomazo<sup>2,4</sup>

<sup>1</sup>UMR CNRS 7193 Institut des Sciences de la Terre de Paris (ISTeP), Sorbonne Université, Paris, France, <sup>2</sup>UMR 6282 Biogéosciences, Université de Bourgogne-Franche Comté, Dijon, France, <sup>3</sup>UMR 7154 Institut de physique du globe de Paris, Université de Paris, Paris, France, <sup>4</sup>Institut Universitaire de France, Paris, France

## OPEN ACCESS

### Edited by:

Eva Stüeken,  
University of St Andrews,  
United Kingdom

### Reviewed by:

Jean-Carlos Montero-Serrano,  
Université du Québec à Rimouski,  
Canada  
Xin-Yuan Zheng,  
University of Minnesota Twin Cities,  
United States

### \*Correspondence:

Laurent Riquier  
laurent.riquier@sorbonne-  
universite.fr

### Specialty section:

This article was submitted to  
Geochemistry,  
a section of the journal  
Frontiers in Earth Science

**Received:** 30 April 2021

**Accepted:** 19 July 2021

**Published:** 13 August 2021

### Citation:

Riquier L, Cadeau P, Danzelle J, Baudin F, Pucéat E and Thomazo C (2021) The Plenus Cold Event Record in the Abyssal DSDP Site 367 (Cape Verde, Central Atlantic): Environmental Perturbations and Impacts on the Nitrogen Cycle. *Front. Earth Sci.* 9:703282. doi: 10.3389/feart.2021.703282

The Oceanic Anoxic Event 2, at the Cenomanian-Turonian boundary (~93.9 Ma), was an episode of widespread burial of organic matter in marine sediments, underlined by a positive carbon-isotope ( $\delta^{13}\text{C}$ ) excursion observed worldwide. Within this episode of  $\text{O}_2$ -depleted conditions, a short interval of cooling, termed as the Plenus Cold Event, has been recorded in many sites and sections in the northern hemisphere (Tethyan domain, Western Interior Seaway, proto-North Atlantic Ocean). But, its record and its impact on the biogeochemical cycles of carbon and nitrogen in the southern part of Central Atlantic Ocean has not been explored yet. Here, we present a detailed geochemical study of the Deep Sea Drilling Project site 367 (Cape Verde) based on a compilation of previous and new data of carbon and nitrogen isotope signals as well as trace element concentrations. The aim of this study is to better constrain the evolution of oxygenation in the water column and the associated changes in nitrogen cycle before and during the Oceanic Anoxic Event 2 in order to understand the paleoceanographic and environmental consequences of the Plenus Cold Event at one of the deepest site of the Central Atlantic Ocean. Our new dataset improves the resolution of the  $\delta^{13}\text{C}$  curve for this site, and we propose a new chemostratigraphic frame of the carbon excursion allowing for a better identification of the short-term negative carbon isotope excursion associated to the Plenus Cold Event. The detailed evolution of redox-sensitive proxies (Mo, U, V, Fe, Cu, Ni enrichments and  $\text{C}_{\text{org}}/\text{P}_{\text{total}}$ ) and isotopic signals ( $\delta^{13}\text{C}_{\text{org}}$  and  $\delta^{15}\text{N}_{\text{total}}$ ) evidence that this deep site was impacted by this cooling event. While anoxic conditions prevailed in bottom waters before and during the onset of the Oceanic Anoxic Event 2 characterized by euxinic  $\text{NH}_4^+$ -rich water column, this cooling event was accompanied by reoxygenation of the water column, which had affected the behavior of the redox-sensitive elements and caused changes in nitrogen biogeochemical cycling.

**Keywords:** cenomanian, turonian, carbon and nitrogen, trace metal elements, chemocline, reoxygenation

## INTRODUCTION

The Cenomanian-Turonian boundary (CTB, ~93.9 Ma ago) is marked by a major environmental disturbance namely the Oceanic Anoxic Event 2 (OAE-2; Schlanger and Jenkyns, 1976). Among the numerous deoxygenation events developed in oceanic domains during the Jurassic and Cretaceous (Jenkyns, 2010 and references herein), OAE-2 has been extensively studied during the last decades because it is one of the most intense and most widespread event, and because of its particularly well preservation in the sedimentary record.

The geological evidence of this event lies primarily on the occurrence of black laminated organic-rich sediments (e.g., black shale) across a wide range of marine settings, ranging from deep ocean basins to shallow shelfal seas. The widespread deposition of these black shales is associated to a short-term (<1 Myr) perturbation of the carbon cycle marked in the case of OAE-2 by a positive carbon-isotope excursion (CIE) recorded in both the organic ( $\delta^{13}\text{C}_{\text{org}}$ , up to 6.0‰) and inorganic ( $\delta^{13}\text{C}_{\text{carb}}$ , up to 2.5‰) reservoirs (e.g., Scholle and Arthur, 1980; Schlanger et al., 1987; Arthur et al., 1988; Jenkyns et al., 1994; Kuypers et al., 2002; Tsikos et al., 2004; Bowman and Bralower, 2005; Erbacher et al., 2005; Sageman et al., 2006; Jarvis et al., 2011; Gale et al., 2019; Danzelle et al., 2020). The positive CIE, resulting from preferential burial of  $^{12}\text{C}$ -rich organic carbon in marine sediments and observed in many marine DSDP-ODP-IODP sites and continental sections and cores, is used to define the extent of the biogeochemical OAE-2 (Gale et al., 1993; Kuypers et al., 2002).

This increased sedimentary organic matter (OM) burial rate is usually argued to reflect increasing nutrient delivery at basin scales leading to increasing primary productivity subsequently transferred to the sedimentary record by deposition of organic-rich deposits. Among possible drivers responsible for this increase in nutrient inputs, an accelerated hydrological cycle is frequently suggested as the leading hypothesis (Arthur et al., 1988; Jenkyns et al., 1994; Kuypers et al., 1999; Jarvis et al., 2011; van Helmond et al., 2014b). This intensification of the hydrological cycle, favoring continental weathering, is due to greenhouse conditions including high temperatures, high atmospheric  $p\text{CO}_2$ , and increases in humidity, as observed at the onset of the OAE-2 (Jarvis et al., 2011). This greenhouse paleoclimate has been directly related to intense volcanic activities associated to emplacement of submarine large igneous provinces (Caribbean and High-Artic) releasing vast quantities of  $\text{CO}_2$  into the ocean and atmosphere (Sinton and Duncan, 1997; Jones and Jenkyns, 2001; Snow et al., 2005; van Bentum et al., 2012; Jenkyns et al., 2017). Seafloor hydrothermalism, associated with these large igneous provinces, and subaerial volcanism may also have supplied nutrients such as metals into seawater reservoirs, sustaining higher primary productivity (Orth et al., 1993; Kuroda et al., 2007; Turgeon and Creaser, 2008; Zheng et al., 2013; Du Vivier et al., 2015; Holmden et al., 2016). As a direct consequence of vigorous and sustained primary productivity, a profound deoxygenation of the water column in many parts of the world ocean, but particularly well expressed in the proto-North Atlantic and in the Central Atlantic (e.g., Sinninghe

Damsté and Köster, 1998; Pearce et al., 2009; Jenkyns, 2010; van Helmond et al., 2014a; Westermann et al., 2014), is recorded in several biogeochemical cycling of elements including but not limited to nitrogen, sulfur, iron and trace metals such as molybdenum or uranium (Brumsack, 2006; Junium and Arthur, 2007; Owens et al., 2012, 2013; Ruvalcaba Baroni et al., 2015). Bottom water anoxia possibly affected up to 50% of the global ocean with local occurrences of euxinic conditions (Monteiro et al., 2012; Owens et al., 2013; Ostrander et al., 2017).

The positive CIE, associated with the OAE-2, is however interrupted by a short-term negative anomaly registered in many sites and sections and referred to as the Plenian carbon isotope excursion (P-CIE; O'Connor et al., 2020). The global distribution of this isotopic carbon anomaly argues for a global change of the carbon cycle. Based on  $p\text{CO}_2$ -dependent proxies ( $\Delta^{13}\text{C}$ ; stomatal index, leaf-wax  $\delta^{13}\text{C}$ ), the P-CIE has been interpreted as a short episode of  $p\text{CO}_2$  rise during the  $\delta^{13}\text{C}$  fall, followed by a decrease in  $p\text{CO}_2$  up to the  $\delta^{13}\text{C}$  maximum value (Kuypers et al., 1999; Sinninghe Damsté et al., 2008; Barclay et al., 2010; Sinninghe Damsté et al., 2010; Jarvis et al., 2011; Danzelle et al., 2020). These rapid oscillations of  $\text{CO}_2$  concentration are thought to be linked to changes in temperature and oxygenation in oceanic domain. Geochemical evidences of oscillations in the oxygenation state of the water column include decrease in OM content and changes in the concentrations of redox-sensitive trace elements (RSTE: Mo, U, V, Cu) recorded within the P-CIE (Jarvis et al., 2011; van Helmond et al., 2014a; Clarkson et al., 2018; Danzelle et al., 2018, 2020; Gale et al., 2019). The reoxygenation interval is usually termed the benthic oxic zone and marked by repopulation of benthic fauna (Friedrich et al., 2006; Keller et al., 2008; Eldrett et al., 2014). The climatic perturbation is associated to the Plenian Cold Event (PCE; Gale and Christensen, 1996). This event, initially highlighted by the incursion of boreal marine fauna into the mid-latitude basins (Vocontian Basin, SE France; Jefferies, 1962; Jefferies, 1963), is now well defined in several basins and at all latitudes (see review of O'Connor et al., 2020 and references herein). The PCE is coeval to the second buildup of the  $\delta^{13}\text{C}$  signal within the positive CIE and has been geochemically characterized by positive isotopic excursion of the  $\delta^{18}\text{O}$  signal and by a decrease of dedicated biomarkers concentrations, such as the crenarchaeotal membrane lipid, linked to the  $\text{TEX}_{86}$ , a sea-surface temperature proxy (Jenkyns et al., 1994; Paul et al., 1999; Tsikos et al., 2004; Forster et al., 2007; Sinninghe Damsté et al., 2008; Takashima et al., 2009; Danzelle et al., 2020). The origin of this short-term carbon cycle event is still debated (atmospheric vs. oceanographic; regional vs global processes) because the triggering factors of  $\text{CO}_2$  change are difficult to identify. The rise in  $p\text{CO}_2$  is thought to be linked to the incursion of a cold oxygenated water mass in tropical to equatorial zones, associated to modification of oceanic circulation (Jenkyns et al., 2017). This oceanographic change would lead to the remineralization of buried OM, which may cause trace metals released from the sediments into the water column and acidification. The PCE has been largely argued to reflect a drawdown in atmospheric  $p\text{CO}_2$  of about 20–25% (Freeman and Hayes, 1992; Jarvis et al., 2011) with extreme estimate up

to 40–80% (Kuypers et al., 1999), resulting from a negative feedback caused by the combination of increased organic carbon burial, CO<sub>2</sub> consumption due to enhanced silicate weathering (Arthur et al., 1988; Sinninghe Damsté et al., 2010; Blättler et al., 2011; Jarvis et al., 2011; Pogge von Strandmann et al., 2013; Jenkyns et al., 2017) and potential cessation of volcanic outgassing (Kuroda et al., 2007).

While a causal relationship between carbon-cycle dynamics and cooling during the PCE is therefore largely documented and argued, especially in mid-latitude zones, little is known on the related biogeochemical cycle of nitrogen at this level of temporal resolution. Meanwhile, previous studies on the nitrogen isotopes record of OM during OAE-2 have proposed several hypotheses to explain commonly observed decrease in sedimentary  $\delta^{15}\text{N}_{\text{total}}$  values such as depth variations of water column chemocline, hence activity and locus of nitrogen fixers and denitrifiers guilds (Kuypers et al., 2002; Junium and Arthur, 2007; Higgins et al., 2012) or changes in the pathway of diazotrophy (from canonical Mo-nitrogenase to alternative V-Fe or Fe-only nitrogenases; Zhang et al., 2014). According to the short residence time of fixed N in modern seawater (<3 kyr) (Tyrrell, 1999; Brandes and Devol, 2002) and to the estimated duration of the P-CIE ca. ~105 kyr (Charbonnier et al., 2018) comprising the ~40–60 kyr PCE as estimated for the boreal sites (Jarvis et al., 2011), high-resolution  $\delta^{15}\text{N}_{\text{total}}$  record of the OAE-2 may offer a chance to better characterized the impact of rapid swings in temperatures on the nitrogen biogeochemical cycle. Moreover, within the context of the greenhouse OAE-2, the short lived PCE provides a unique opportunity to testify the hypothesis of Algeo et al. (2014), who proposed that the link between high temperatures and low  $\delta^{15}\text{N}_{\text{total}}$  values observed on long times scale during greenhouse intervals may be potentially also observed during shorter event such as OAEs and should reflect lower integrated water-column denitrification rates in comparison to icehouse intervals.

Among the several sites, where the OAE-2 and the PCE has been recorded, the Deep Sea Drilling Project (DSDP) site 367 (Leg 41, Cape Verde, Central Atlantic) represents an interesting study case, characterized by a positive CIE of 6.0‰ (Arthur et al., 1988) and by a noticeable enrichment of organic carbon (up to 45%; after Herbin et al., 1986) deposited in abyssal environment in low latitude zone. Previous studies, mainly based on  $\delta^{13}\text{C}$  and  $\delta^{15}\text{N}_{\text{total}}$  isotopic signatures and biomarker identifications (Kuypers et al., 2002, Kuypers et al., 2004; Sinninghe Damsté et al., 2008), organic paleothermometer TEX<sub>86</sub> (Schouten et al., 2003; Forster et al., 2007), iron speciation,  $\delta^{56}\text{Fe}_T$ ,  $\delta^{98/95}\text{Mo}$  isotopic signatures (Owens et al., 2012; Westermann et al., 2014; Dickson et al., 2016) and some trace element concentrations (Kuypers et al., 2002; Westermann et al., 2014) have been already realized on a few samples (14–17, except for Dickson et al. (2016), which was realized on 114 samples from the archive of half of the core) of this deep-water site. An integrated and detailed work is however needed to better constrain the primary signal of geochemical proxies, to reconstruct the paleo-environmental conditions during the OAE-2 and the PCE and to determine the impact of this event on the nitrogen cycle in one of the deepest settings of the CTB.

The aim of this work is thus to 1) achieve a detailed study of the OAE-2 in deep-sea context based on a multi-proxy study (including  $\delta^{13}\text{C}_{\text{org}}$ ,  $\delta^{15}\text{N}_{\text{total}}$ , Rock-Eval and trace metals) of the DSDP 367 succession from Cape Verde, and 2) propose a model that account for the evolution of the biogeochemical cycle of nitrogen and its relation to environmental perturbations for the southeastern part of the Central Atlantic.

## MATERIAL AND METHODS

### Sampling Location

Site 367 (12°29.2'N; 20°02.8'W) was drilled in 1975 during the DSDP Leg 41 and is located off the coast of the Senegal in the Cape Verde Basin (Figure 1). This site shows an almost continuous sedimentary record from Upper Jurassic (Oxfordian-Kimmeridgian) up to Pleistocene (Lancelot et al., 1978). During the Cretaceous, this site belonged to the southern part of the Central Atlantic and a paleodepth of around 3,700 m has been estimated based on isostatic methods (Chenet and Francheteau, 1979). Thus, sediments were deposited in abyssal plain environment, probably below the Carbonate Compensation Depth (even if some traces of carbonate do exist, Chenet and Francheteau, 1979).

The studied succession, composed of cores 19 and 18, is about 13.5 m thick (from 650 to 636.5 m depth), with a coring hiatus of 2.2 m from 645.7 to 643.5 m depth. The sedimentary sequence is mainly composed of laminated black shales and terrigenous silicates. In details, in core 19, green and olive-grey calcareous clays are interbedded with laminated black shales whereas the core 18 is dominantly composed of laminated black shales, especially in the sections 5 and 1 (Mélières, 1978; Herbin et al., 1986). In some studied samples, some strong post-depositional oxidation of the pyrite within the sediments has been noticed and is underlined by the presence of abundant jarosite and iron oxides.

### Methods

A total of 42 rock samples were collected every 5–20 cm according to sample availability as following: seven from the base of the studied interval up to the void (650.5–647.7 m depth) and 35 above the void (643.3–636.5 m depth). After cleaning, all rock samples were powdered manually in an agate mortar, at the Biogeosciences Laboratory of the University of Burgundy in Dijon (France).

### Carbon and Nitrogen Analyses

Concentration and isotopic composition of organic carbon ( $\text{C}_{\text{org}}$ ,  $\delta^{13}\text{C}_{\text{org}}$ ) and total nitrogen ( $\text{N}_{\text{total}}$ ,  $\delta^{15}\text{N}_{\text{total}}$ ) were measured on carbonate free residues. Sample powders were rinsed by dichloromethane-ethanol (9:1) to remove any modern organic contaminant and reacted with hydrochloric acid (HCl; 6N) at room temperature overnight followed by 4 h at 80°C to remove carbonate phases. The residues were rinsed with deionized distilled water and centrifuged several times until neutral pH was reached and then dried at 60°C overnight in an oven. Aliquots of carbonate free samples (30–60 mg) were then weighed and

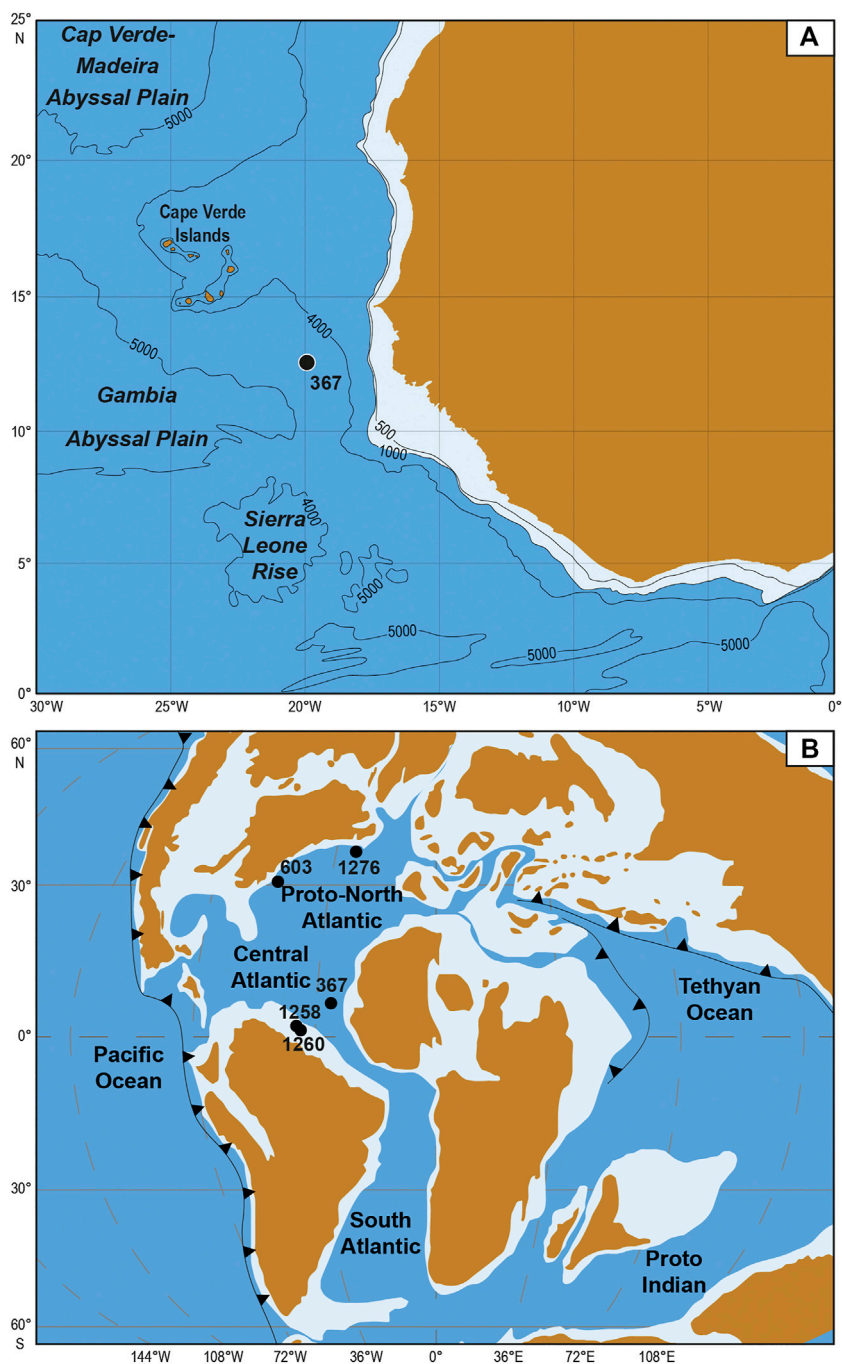


**FIGURE 1** | Location of the DSDP site 367 in the Cape Verde Basin (modified from Lancelot et al., 1978) **(A)** and paleomap of the Cenomanian-Turonian Central Atlantic and proto-North Atlantic zones with the paleopositions of the site 367 and other DSDP/ODP sites (603, 1258, 1260, and 1276) mentioned in this paper (van Hinte et al., 1993; Erbacher et al., 2004a, Erbacher et al., 2004b; Tucholke et al., 2004) **(B)**.

poured in tin capsules. Isotopic measurements were performed at the Biogeosciences Laboratory, Dijon (France), on a vario Micro cube elemental analyser (Elementar) coupled to an IsoPrime stable isotope ratio mass spectrometer (Isoprime) in continuous flow mode. The carbon and nitrogen isotopic compositions are both expressed in delta notation and

reported as the per mil (‰) deviation relative to the Vienna Pee Dee Belemnite (VPDB) standard for carbon and to AIR standard for nitrogen. USGS40 certified reference material (C = 40.8 wt%; N = 9.52 wt%;  $\delta^{13}\text{C}_{\text{VPDB}} = -26.39\text{‰}$ ,  $\delta^{15}\text{N}_{\text{AIR}} = -4.52\text{‰}$ ) was used for calibration. The organic carbon ( $\text{C}_{\text{org}}$ ) and total nitrogen ( $\text{N}_{\text{total}}$ ) content is expressed as dry weight



**TABLE 1** | Correlation factor *r* between Al and major and minor elements.

	Fe	Mn	P	Si	Ba	Co	Cr	Cu	Mo	Ni	Th	U	V	Zn	Zr
Al	0.00	0.17	-0.45	0.96	-0.30	0.06	0.77	0.15	-0.65	-0.65	0.97	-0.68	0.03	0.02	0.93

percentage (wt%) of the total fraction. From these values, the molar  $C_{org}/N_{total}$  ratio was calculated. The external reproducibility based on duplicate analyses of carbonate free samples was better than  $\pm 0.15$  wt% ( $1\sigma$ ) for carbon and  $\pm 0.10$  wt% ( $1\sigma$ ) for nitrogen. External reproducibility based on duplicate analyses of the samples was better than  $\pm 0.05\%$  and  $\pm 0.5\%$  for carbon and nitrogen, respectively.

### Rock-Eval Pyrolysis

Organic matter parameters, including Total Organic Carbon (TOC) content, Hydrogen Index (HI), Oxygen Index (OI) and temperature of the maximum yield of hydrocarbon ( $T_{max}$ ) were obtained using 10–50 mg of bulk powder, on a Rock-Eval 6 Turbo at the ISTE P Laboratory of Sorbonne University in Paris (France), by sequential pyrolysis and oxidation treatment (Espitalié et al., 1985a; Espitalié et al., 1985b; Espitalié et al., 1986; Lafargue et al., 1998; Behar et al., 2001). Reproducibility was evaluated by replicates analyses of laboratory standards and was better than  $\pm 0.05$  wt% ( $1\sigma$ ) for TOC,  $\pm 1.5^\circ\text{C}$  ( $1\sigma$ ) for  $T_{max}$ ,  $\pm 10$  mg HC/g TOC ( $1\sigma$ ) for HI, and  $\pm 10$  mg  $\text{CO}_2/\text{g}$  TOC ( $1\sigma$ ) for OI. The TOC (%) concentration, obtained by whole-rock analyses from the Rock-Eval method, is in agreement with this of  $C_{org}$ , determined on the carbonate-free fraction ( $r = 0.97$ ) and show similar vertical distribution but with lower value compared to  $C_{org}$  (except for one sample).

### Analysis of Major and Trace Elements

Major and trace elements analyses were performed using inductively coupled plasma mass spectrometry (ICP-MS) at the Activation Laboratory (Actlab) in Ancaster, Canada. Protocol information for the package 4Litho-Lithium Metaborate/Tetraborate Fusion ICP and ICP-MS can be found at [www.actlabs.com](http://www.actlabs.com). Reproducibility is better than 2% of the measured values ( $1\sigma$ ) for major and trace elements.

To eliminate a possible detrital origin of selected elements (Ba, Co, Cr, Cu, Mo, Ni U, V, Zn Fe, Si, and P), the Al concentration was linearly correlated with each element and correlation coefficient *r* was calculated (Table 1). Aluminum is considered as an indicator of the aluminosilicate contribution to the sediments and is also a conservative element during secondary processes. For most of them (except for Si, Th, Zr and to a lesser extent Cr), no noticeable correlation or anti-correlation is observed, suggesting a non-detrital (i.e., authigenic) origin. In order to compare values obtained in this work with those of previous studies and from other Central and proto-North Atlantic sites, the concentration of major and trace elements were normalized to aluminum (El/Al) to correct for dilution effects by varying carbonate or OM contents. It is important to note here that although Al concentrations are always upper than 1%, fluctuating from 1.2 to 6.6%, they show a progressive decreasing trend from the base to the top of the studied

interval (see **Supplementary Material**). So, for few samples, mainly located in the upper part of the studied sections (638.1; 638.7 and 640.35 m) and characterized by the lowest concentration of Al (<1.5%), normalization may lead to a slight exaggeration of El/Al values.

Lastly, the enrichment factor (EF) was also calculated following the formula:  $EF = (\text{Element}/\text{Al})_{\text{sample}}/(\text{Element}/\text{Al})_{\text{reference}}$ . This reference could be either the Post-Archean Average Shales (PAAS, Wedepohl, 1971) or the Upper Continental Crust (UCC, McLennan, 2001). For this work, the EFs were calculated using the UCC concentrations. As precised by Algeo and Tribovillard (2009),  $EF > 3$  represents a detectable authigenic enrichment, whereas  $EF > 10$  represents a substantial authigenic enrichment.

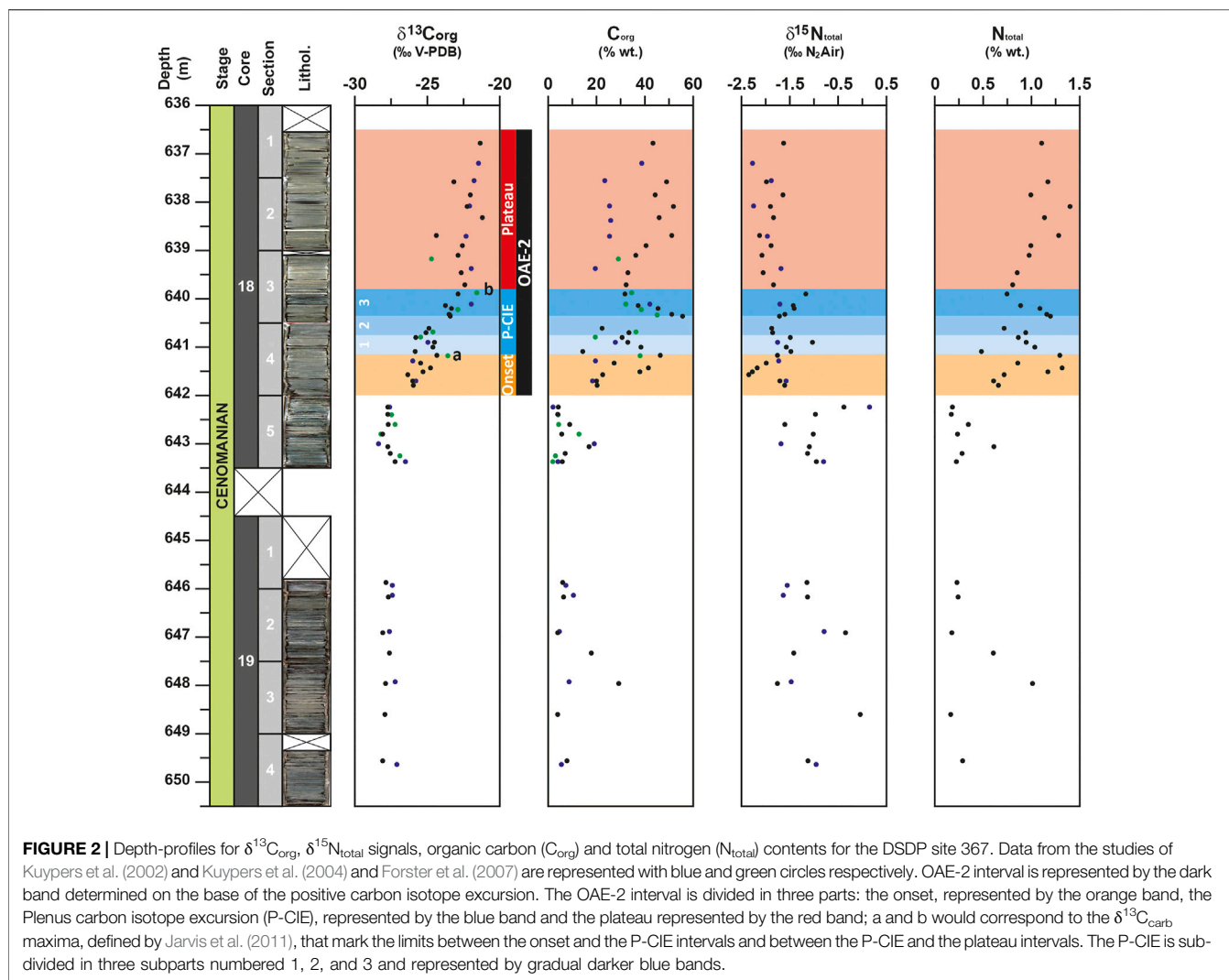
## RESULTS

In order to have the highest resolution for geochemical signals, the results obtained in this study ( $n = 42$ ) have been compiled with those of previous studies ( $n = 17$  from Kuypers et al., 2002, Kuypers et al., 2004 and from H-J., Brumsack, unpublished data, for selected major and trace elements (Fe, Mn, P, Ni, Cu, Co, and Zn) on the same 17 samples;  $n = 29$  from Forster et al., 2007 and  $n = 14$  from Westermann et al., 2014).

### Stable Isotopes

The  $\delta^{13}C_{org}$  values of this study range from  $-28.5$  to  $-21.2\%$  (Figure 2) and are in agreement with the data reported by Kuypers et al. (2002) completed by Forster et al. (2007) for this site. After a phase of stability at the base of the section (649.6–642.0 m) with  $\delta^{13}C_{org}$  values of  $\sim -27.8\%$ , an increasing trend of about  $+3.5\%$  is observed up to 641.15 m, where  $\delta^{13}C_{org}$  value reaches up to  $-24.3\%$ . This first increase is followed by a 1.45 m thick interval marked by lower values down to  $-25.8\%$  at 640.8 m and a second phase of  $\delta^{13}C_{org}$  increase with values up to  $-22.4\%$  recorded at 639.7 m. A short plateau interrupts this second rapid increase with values close to  $-23.5\%$  around 640.35 m. Upward (639.7–636.5 m),  $\delta^{13}C_{org}$  values remain high oscillating between  $-22.5$  and  $-21.2\%$ .

The  $\delta^{15}N_{total}$  record of this study shows negative values ranging from  $-2.3$  to  $-0.4\%$ , which also compare well to the  $\delta^{15}N_{total}$  record of Kuypers et al. (2004) for this site (Figure 2). Unlike the  $\delta^{13}C_{org}$ , the  $\delta^{15}N_{total}$  profile does not show interval of stable values at the base of the studied core. From 649.6 to 645.9 m and from 643.4 to 642.2 m,  $\delta^{15}N_{total}$  values oscillate between  $-1.7$  and  $0.0\%$  and between  $-1.6$  and  $-0.4\%$ , respectively. It is important to note here that maximum value of  $\delta^{15}N_{total}$  is reached at the base of the OAE-2, when  $\delta^{13}C_{org}$  values are yet low. The rest of the studied core is characterized by lower  $\delta^{15}N_{total}$  with values down to  $-1.5\%$ . However, unlike to



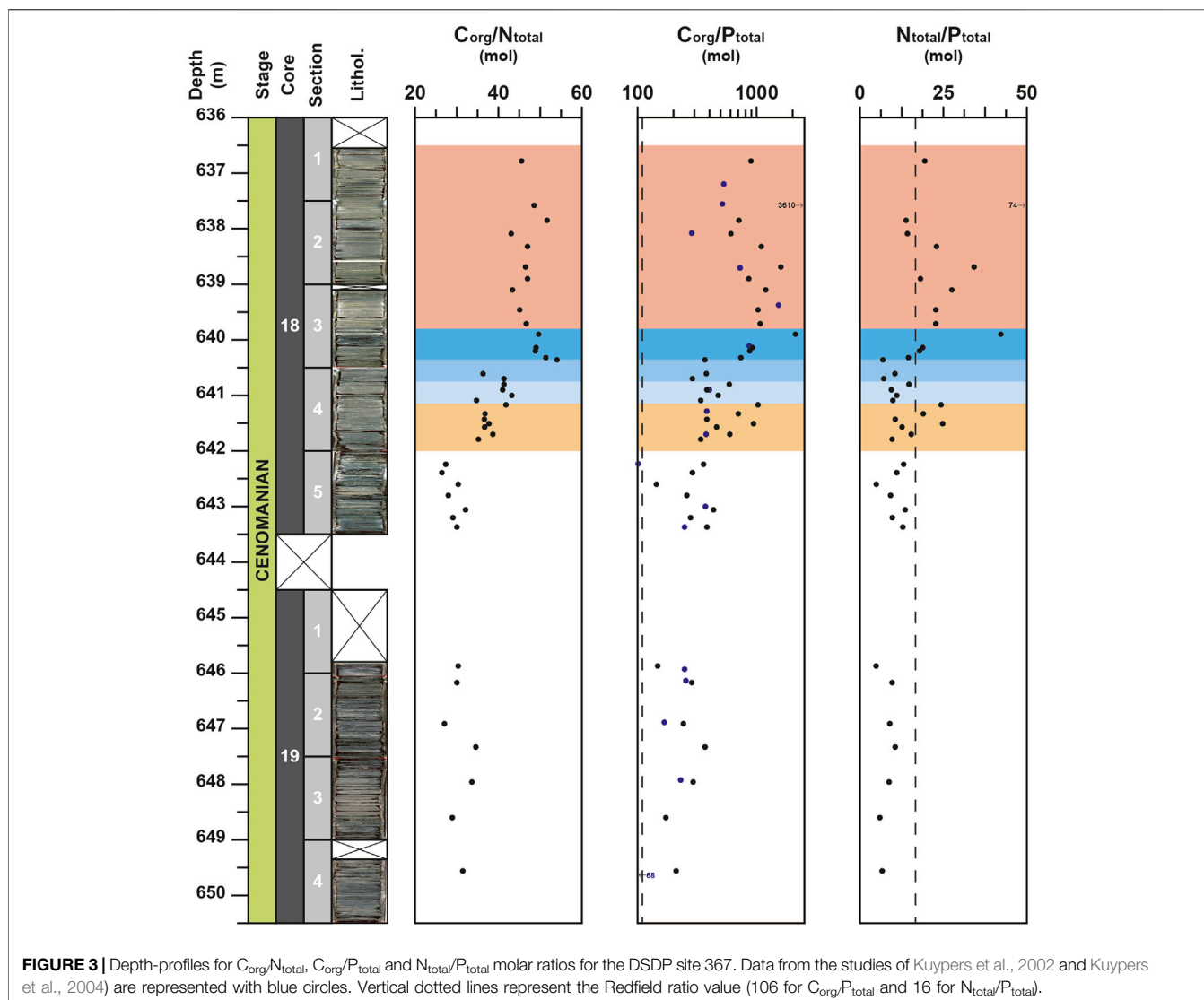
the  $\delta^{15}\text{N}_{\text{total}}$  signal from Kuypers et al. (2004), which did not record noticeable variation from 642.0 to 636.5 m, two intervals can be recognized in the more detailed  $\delta^{15}\text{N}_{\text{total}}$  record of this study. During the first interval (641.8–639.9 m),  $\delta^{15}\text{N}_{\text{total}}$  values oscillate between  $-2.3$  and  $-1.0$ ‰, then from 639.7 to 636.5 m, a second interval of low  $\delta^{15}\text{N}_{\text{total}}$  values ( $\sim -1.9$ ‰) is recognized. In more details, the 1.9 m thick first interval (641.8–639.9 m) records a succession of two negative and two positive excursions of the  $\delta^{15}\text{N}_{\text{total}}$ . The first negative excursion of  $\delta^{15}\text{N}_{\text{total}}$  broadly corresponds to the first buildup of  $\delta^{13}\text{C}_{\text{org}}$  signal, the two positive excursions are recorded at the base and at the top of the 1.5 m thick interval marked by a slight trough and a second phase of rapid change in  $\delta^{13}\text{C}_{\text{org}}$  values, corresponding to the P-CIE.

## Carbon, Nitrogen, and Phosphorus Contents

In the core 19, the  $\text{C}_{\text{org}}$  profile is marked by a noticeable peak up to 29.3% at 648.0 m (Figure 2). At the base of the core 18, a slight

increase of  $\text{C}_{\text{org}}$  values up to 17% is observed around 643.0 m. Similar trend with  $\text{C}_{\text{org}}$  values up to 20% was previously recorded for this site by Kuypers et al. (2002) and Forster et al. (2007). This is followed by a short interval of low values (down to 4% at 642.25 m) and a progressive increase of  $\text{C}_{\text{org}}$  values up to 46.4% at 641.2 m. After an episode of oscillating values, a short interval with the highest  $\text{C}_{\text{org}}$  values (between 45.5 and 55.5%) is recorded from 640.35 to 640.2 m, followed by a rapid decrease down to 31.8% recorded at 639.9 m. Lastly, a progressive increasing trend followed by a second interval of high  $\text{C}_{\text{org}}$  values (between 43.4 and 51.8%) is recorded from 638.7 m up to the end of the studied section. This second increasing trend and associated high values of  $\text{C}_{\text{org}}$  were not observed in Kuypers et al. (2002) and Forster et al. (2007). In these studies, a plateau of values around 25% marked this interval. The  $\text{N}_{\text{total}}$  profile, which oscillates from 0.16 to 1.40%, shows a similar evolution than the  $\text{C}_{\text{org}}$  ( $r = 0.97$ ) with high values ( $>0.8\%$ ) recorded at 648.0 m in the core 19 and from 641.5 m onward in the core 18 (Figure 2).

The  $\text{C}_{\text{org}}/\text{N}_{\text{total}}$  ratio shows high values when compared to the Redfield ratio (i.e.  $106/16 = 6.625$ , Redfield, 1958) and range



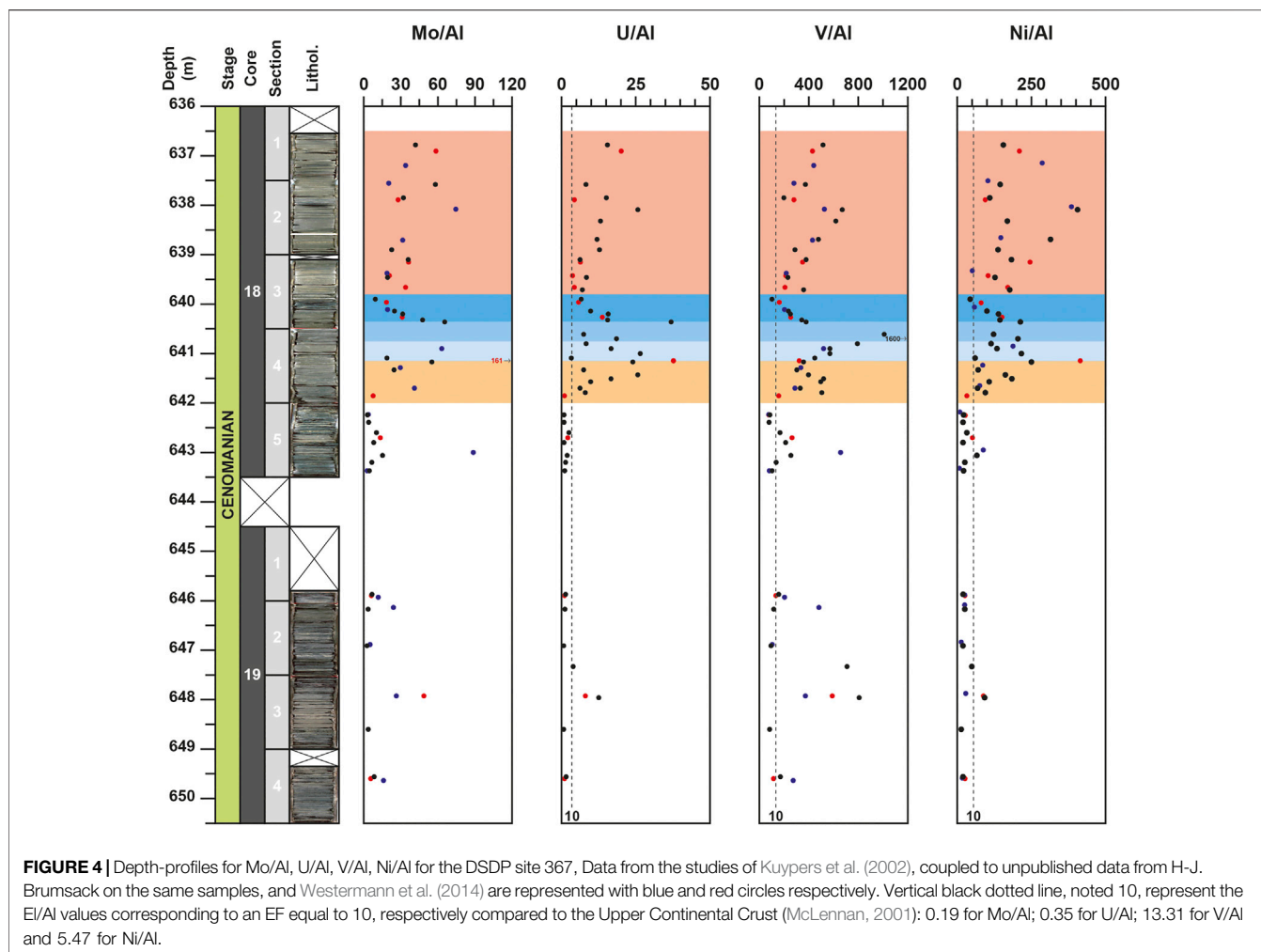
between 26 and 54 (**Figure 3**). This range of values is comparable to those (25–50) usually recorded in Cretaceous black shale deposits (Rau et al., 1987; Junium and Arthur, 2007). Moreover, similar to the  $\delta^{13}C_{org}$ , the  $C_{org}/N_{total}$  profile shows three distinguished intervals in the studied cores. From 649.60 to 642.25 m, all values are lower than 35, then upward a noticeable increase the  $C_{org}/N_{total}$  ratio is recorded with the highest value (54) reached at 640.35 m. From this depth onward, the  $C_{org}/N_{total}$  values remain high oscillating between 43 and 52.

For the  $C_{org}/P_{total}$  molar ratio, all values are higher than the Redfield ratio ( $C_{org}/P_{total} = 106$ ). In detail, the signal remains relatively constant from the base of the studied section up to 641.8 m with average value of 280. Then, an increasing trend is observed from 641.8 m up to 639.9 m, where the  $C_{org}/P_{total}$  molar ratio reaches 2093 (**Figure 3**). For the rest of the section, the  $C_{org}/P_{total}$  values tend to decrease but two noticeable peaks of 1,590 and 3,610 are recorded at 638.7 and 637.6 m, respectively.

The  $N_{total}/P_{total}$  molar ratio shows similar variations than the  $C_{org}/P_{total}$  molar ratio ( $r = 0.99$ ). From 649.5 to 640.25 m, the  $N_{total}/P_{total}$  values are nearly constant with average values close to 10 (**Figure 3**). Only two peaks up to 24, due to increasing N content, are recorded at the base of the OAE-2 (at 641.5 and at 641.2 m). From 640.20 m onward, the  $N_{total}/P_{total}$  values sensibly increase, with most values exceeding the canonical Redfield ratio (i.e.,  $N_{total}/P_{total} = 16$ ).

## Major and Trace Element Evolutions

Compared to the values of the UCC (McLennan, 2001), all the elements that are not linked to detrital fraction exhibit noticeable enrichment. The element to Al (El/Al) ratios exhibit contrasted evolutions depending on the considered element. For the core 19, most of elements record a positive peak of concentration and ratio at 648.0 m. This peak is particularly well expressed for U, V, Cd, Cu, and Zn (**Figures 4,5**) and corresponds to high  $C_{org}$  values (up to 29.3%).



For the core 18, after a slight enrichment recorded around 643.0 m for only few elements (Mo, V, Ni, Zn, Ba), which was also observed in previous studies (Kuypers et al., 2002; Westermann et al., 2014), most elements are characterized by noticeable enrichments starting at 642.0 m and by an interval with the highest values from 640.8 to 640.35 m (Figures 4–6). This 45 cm-thick interval is well observed in the Al-normalized profiles of P, Cu, Zn, V, U, and Cd and corresponds to the highest values of  $C_{org}$  (up to 55.5%). Compared to previous studies (Kuypers et al., 2002; Westermann et al., 2014), the results obtained here allow to highlight for the first time this noticeable enrichment of these elements around 640.5 m depth. For most of them (P, Cu, Zn, V, U and Mo), this is followed by a noticeable decrease of El/Al values up to around 639.0 m depth. For few other elements, such as Ba, Ni, Co, and Fe, the highest values are observed upper in the core. For Ba, noticeable fluctuations are recorded from 642.0 m and the highest value are recorded around 639.0 m, whereas for Ni and Fe, the highest values are observed at 638.1 m and are coeval with peaks in the Al-normalized profiles of P, U, and V (Figures 4–6). Lastly, some elements, like Mn or Zr, do not show noticeable variations in the studied interval. These elements exhibit values mainly lower than

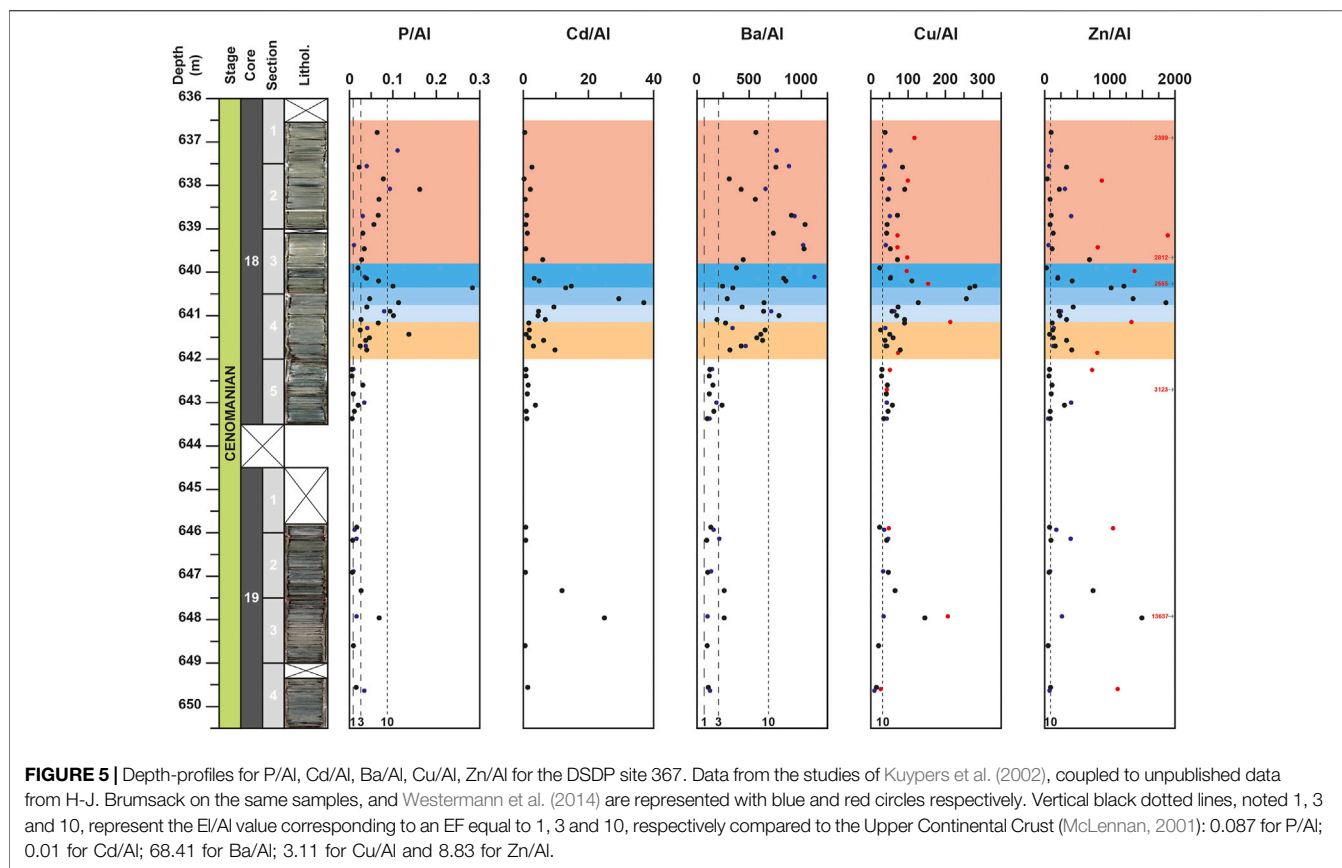
the UCC value or close to it. Only one obvious positive peak at 640.9 m for Mn and a negative peak at 640.35 m for Zr are observed (Figure 6).

## INTERPRETATIONS AND DISCUSSIONS

### Identification of the Plenius Carbon Isotope Excursion Within the Deep Sea Drilling Project Site 367

Since the works of Gale et al. (1993), it is well established that the OAE-2 is defined by a positive stable CIE, composed of several spikes and nudges. This excursion is usually subdivided into three main phases: an earlier phase A, named rapid shift, characterized by an increase in  $^{13}C/^{12}C$  ratio values from the pre-excursion background value and thus by an increase of  $\delta^{13}C$  in both organic and carbonate fractions, a following phase B, corresponding to a plateau of high  $\delta^{13}C$  values, and a final phase C, characterized by a gradual drop of  $\delta^{13}C$  values toward pre-excursions level (Kuypers et al., 2002). As an OAE correspond by definition to the main phase of enhanced isotopically light organic carbon burial

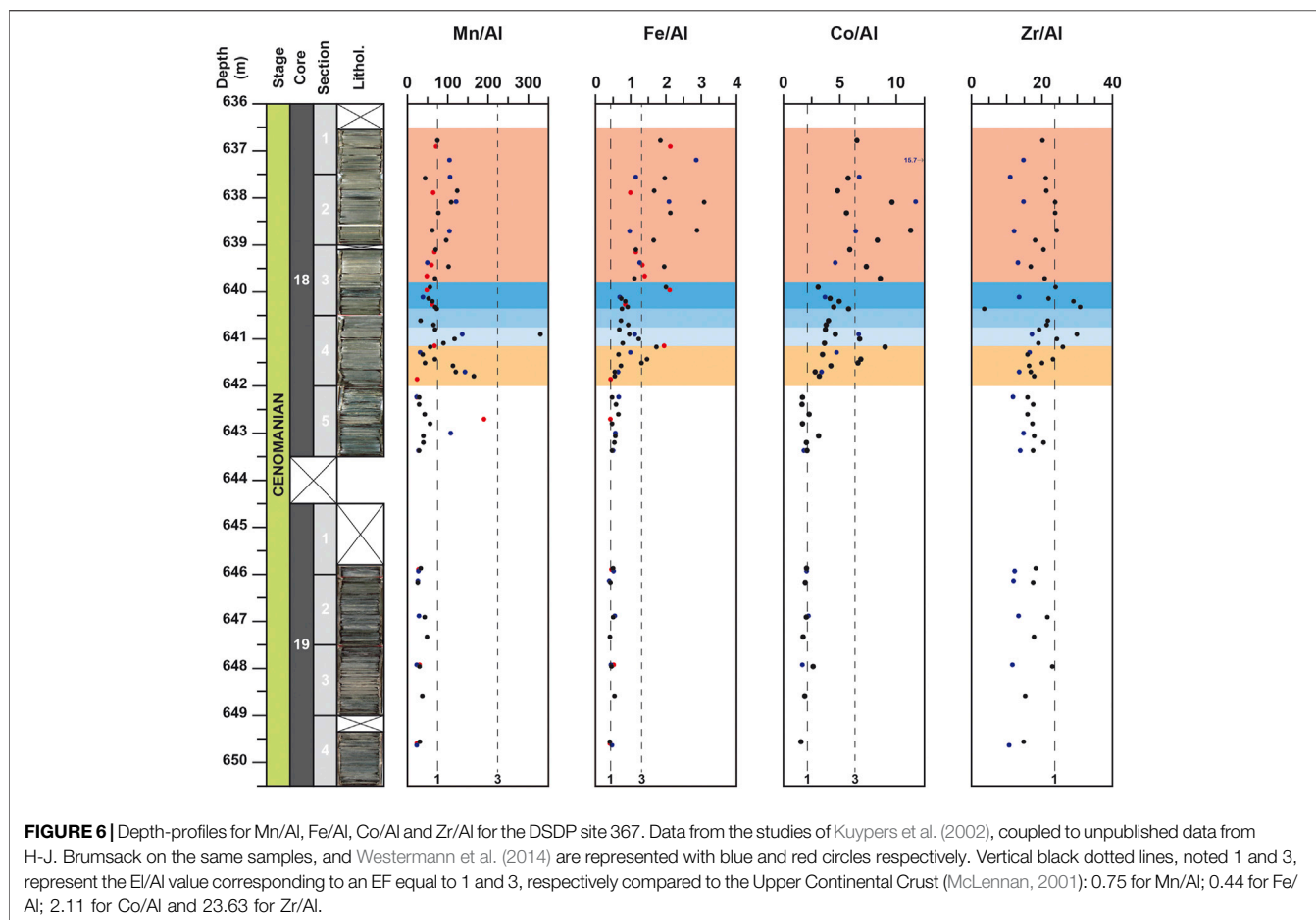




(Arthur et al., 1988), the Cenomanian-Turonian OAE-2 is thus restricted to the phases A and B (Kuypers et al., 2002). In high-resolution isotope profiles, such as measured in Eastbourne (Paul et al., 1999); Lambrousse (Takashima et al., 2009; Danzelle et al., 2020) and Pont d'Issole (Jarvis et al., 2011), the phase A can be further subdivided in three intervals: an initial rise in  $\delta^{13}\text{C}_{\text{carb}}$  value, corresponding to the first buildup, ended by a first maximum value ( $\delta^{13}\text{C}_{\text{carb}}$  maxima a in Jarvis et al., 2011), followed by a slight decrease, associated to a trough interval, and a further rise, corresponding to the second buildup, to the maximum values of the CIE ( $\delta^{13}\text{C}_{\text{carb}}$  maxima b in Jarvis et al., 2011) that define the beginning of the phase B (plateau interval). The short-lived interval, composed by a “trough interval” and the “second build-up”, correspond to the P-CIE (O'Connor et al., 2020). This interval is associated with a cooling event, marked by a southerly incursion of boreal fauna (including the belemnite *Praeactinocamax plenus*, the bivalve *Oxytoma seminudum* and the serpulid worm *Hamulus sp.*) into mid-latitude areas (Jefferies, 1962; Gale and Christensen, 1996) and by positive oxygen isotopic excursion recorded in carbonates (Jarvis et al., 2011). This faunal and paleoclimatic event is referred to as the PCE (Gale and Christensen, 1996) and was identified from a number of paleo-temperature proxies at several European, North America and Atlantic sites. For the DSDP site 367, the PCE has been identified using the organic paleothermometer  $\text{TEX}_{86}$  signal which show low value (0.84) around 640.1 m (Schouten et al., 2003; Forster et al., 2007). In more details, the  $\text{TEX}_{86}$  signal

records a  $\sim 1$  m thick interval (640.35–639.40 m) marked by a negative excursion, interpreted as a sea surface temperature decline of about  $4^\circ\text{C}$  (Forster et al., 2007). Recently, based on low  $\delta^{98/95}\text{Mo}$  values, Dickson et al. (2016) have reported in the same succession an 80 cm thick interval (640.86–640.05 m), slightly deeper to those defined by  $\text{TEX}_{86}$  signal corresponding to the PCE.

In agreement with previously OAE-2 carbon-isotope records (e.g., Paul et al., 1999), five distinctive phases can be recognized in the carbon-isotope signal of the DSDP site 367. The first phase of the  $\delta^{13}\text{C}_{\text{org}}$  signal (649.5–642.0 m), with values clustering around  $-27.8\text{‰}$ , corresponds to the pre-excursion interval. The first rapid shift of  $\delta^{13}\text{C}_{\text{org}}$  values up to  $-24.3\text{‰}$  (642.00–641.15 m) corresponds to the first buildup, which marks the onset of the OAE-2, such as in typical CTB sections, like Eastbourne (Gale et al., 1993) and Pont d'Issole (Jarvis et al., 2011; Danzelle et al., 2018). The following 1.35 m thick interval (641.15–639.80 m) is interpreted as an equivalent of the P-CIE recorded in the Eastbourne section (O'Connor et al., 2020). The first 40 cm of this interval would represent the short trough and is referred here as the PCE-1 (641.15–640.75 m) and the last 95 cm would correspond to the second buildup. In this study, this interval is subdivided in two parts: a 40 cm thick interval referred here as the PCE-2 (640.75–640.35 m) and a 55 cm thick interval referred here as the PCE-3 (640.35–639.80 m). The limit between PCE-2 and PCE-3 corresponds to a short plateau of  $\delta^{13}\text{C}$  values. The top of the core encompasses part of the isotopic plateau,



corresponding to the phase B in Kuypers et al. (2002) and start at 639.80 m. The end of the phase B and the gradual return to pre-excursion values, which marks the CTB and corresponds to the phase C are not recorded in the DSDP site 367.

Based on the new  $\delta^{13}\text{C}$  data, obtained in this study, the onset of the OAE-2 and the phase A should be moved from 643.0 m, as initially proposed by Kuypers et al. (1999), to 642.0 m depth. Even if the lowest values of  $\delta^{13}\text{C}$  signal,  $-28.4\text{‰}$  in Kuypers et al. (1999) and  $-28.1\text{‰}$  in this study are respectively recorded at 643.0 and 642.8 m, the following values do not show noticeable increase before 642 m. They oscillate from  $-27.6$  to  $-27.2\text{‰}$  in Kuypers et al. (1999) and Forster et al. (2007) and are close to  $-27.7\text{‰}$  in this study. The onset of the  $\delta^{13}\text{C}_{\text{org}}$  shift is observed by a noticeable increase of  $1.8\text{‰}$  between 642.25 and 641.8 m in this study and 641.7 m in Kuypers et al. (1999). The A/B limit, marked by the first highest value of  $\delta^{13}\text{C}$  recorded after the PCE, is located before 640 m, probably close to 639.8 m rather than at 640.1 m, as initially proposed by Kuypers et al. (2002). This new evolutionary frame agrees with data reported by Forster et al. (2007), which record the highest value of  $\delta^{13}\text{C}_{\text{org}}$  of  $-21.6\text{‰}$  at 639.9 m. Our results confirm that, as in other sites, the cooling, associated to the PCE, started after the onset of the P-CIE and the lowest temperature is recorded close to the isotopic A/B limit.

### Organic Matter Source and Maturity

Both the  $\text{C}_{\text{org}}$  (%) and TOC (%) values calculated from carbonate free fraction and from bulk-rock by Rock-Eval pyrolysis show important enrichment of OM content (up to 55%, at 640.35 m). In both signals, a noticeable increase of organic carbon content, coeval with the onset of OAE-2 and associated with the  $\delta^{13}\text{C}_{\text{org}}$  positive excursion, is observed from 642.0 m.

As shown in the modified van Krevelen diagram (Figure 7A), most samples have HI values higher than 400 mg HC/g TOC and are characterized by low OI values, which never exceed 65 mg  $\text{CO}_2/\text{g TOC}$ . In detail, pre-OAE-2 samples, with TOC mostly lower than 10%, record HI values lower than 350 mg HC/g TOC and OI values upper than 45 mg  $\text{CO}_2/\text{g TOC}$ . In the modified van Krevelen diagram, these values plot in the Type II and Type III domain, consisting theoretically of a mix of marine and terrestrial material. However, as demonstrated by previous studies based on molecular fossils (Kuypers et al., 1999; Kuypers et al., 2002; Sinnighe Damsté et al., 2008), OM is thought to have a dominant marine origin, even before the OAE-2. Molecular fossils of unambiguous terrestrial origin (i.e., leaf wax lipids and oleoananes) are present only in low abundance in the extractable OM (Kuypers et al., 2002). For these samples, it is likely that the marine OM had been partially oxidized with a

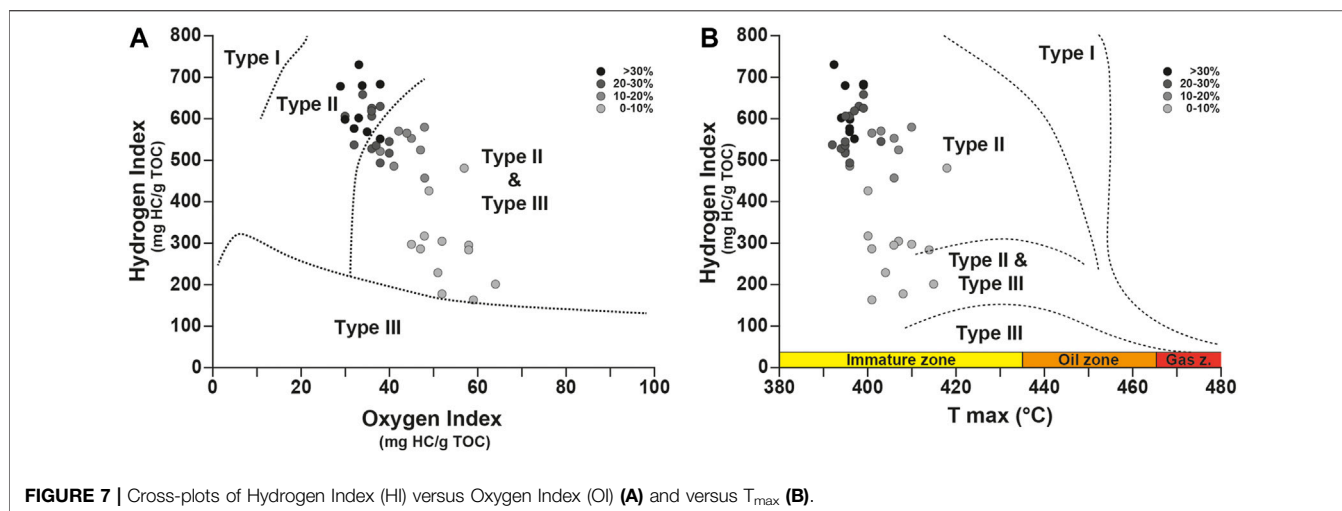


**FIGURE 7** | Cross-plots of Hydrogen Index (HI) versus Oxygen Index (OI) (A) and versus  $T_{max}$  (B).

consequence of a lowering of HI. The samples within the OAE-2 record the highest values of HI (up to 730 mg HC/g TOC) and the lowest values of OI (down to 30 mg CO<sub>2</sub>/g TOC). For these samples, these range of HI and OI values correspond to OM of Type II (marine origin), deriving from algal and bacterial sources. These data confirm the first results obtained by Herbin et al. (1986) on this site. Based on the significant covariation of  $\delta^{13}C_{org}$  with  $\delta^{13}C$  of the extended hopanoids and sulfur-bound phytane ( $r = 0.91$ ), Kuypers et al. (2004) argue for the predominance of cyanobacteria in the phytoplanktonic community and thus in the sedimentary OM. The  $T_{max}$  values oscillate between 392 and 418°C, clearly indicating an immature OM (Figure 7B), hence a shallow burial of sediments. This result is in good agreement with the preservation of molecular fossils (see Kuypers et al., 2002; Sinninghe Damsté et al., 2008) within the studied site and indicates that the burial diagenesis might have been limited.

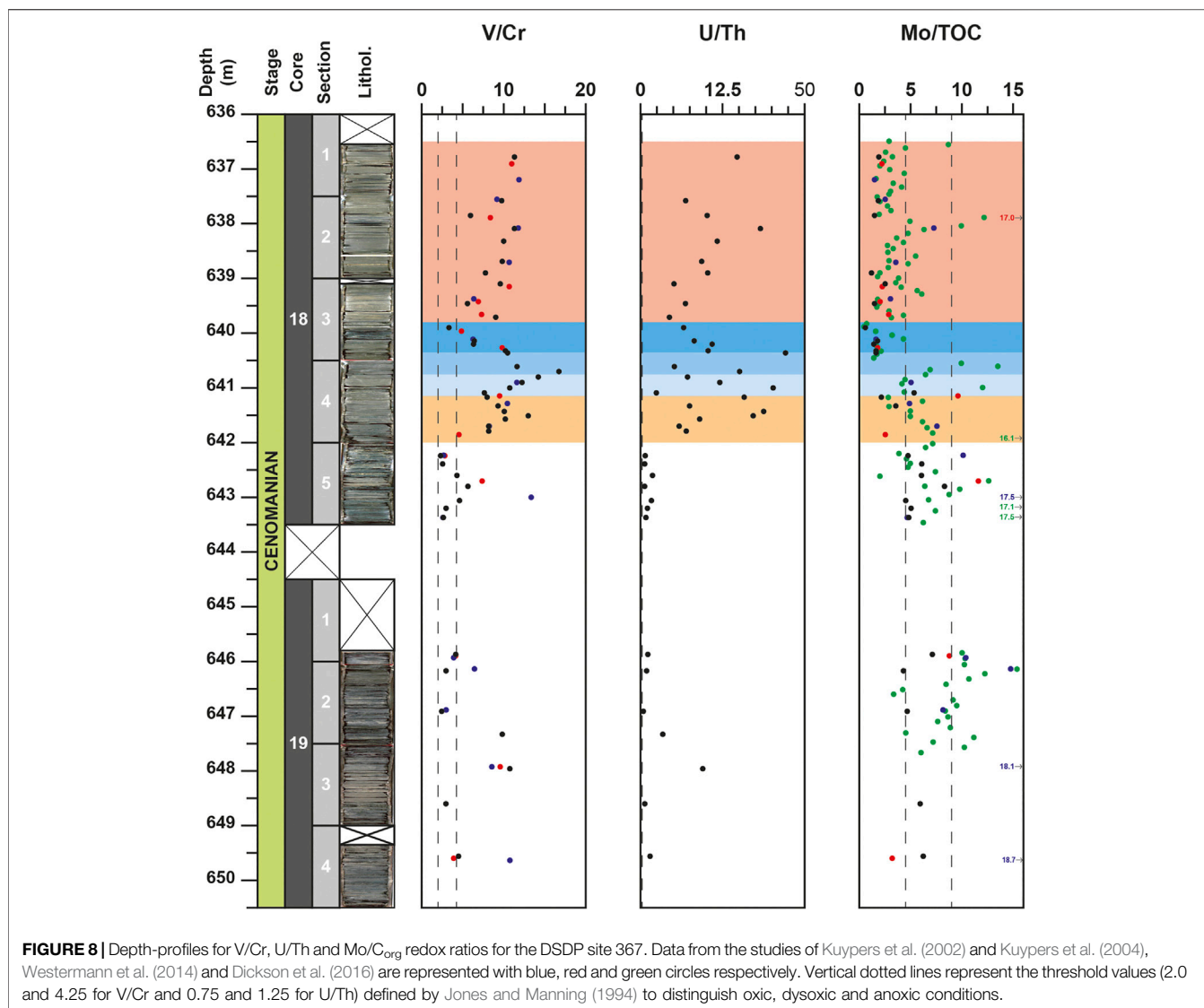
## Evolution of the Oxygenation Conditions and of the Water Mass Restriction During the Oceanic Anoxic Event 2

Among the DSDP-ODP-IODP sites from the Central Atlantic, the DSDP site 367 is usually considered as being continually overlain by anoxic to euxinic water masses during the late Cenomanian times (Dickson et al., 2016). This is based on high value of  $C_{org}/P_{total}$  ratio (mostly >106; up to 1,536) and high values of Mo concentration (mostly >40 ppm and up to 630 ppm) obtained from previous studies (van Helmond et al., 2014a; Dickson et al., 2016). Occurrence of isorenieratene and chlorobactene, two biomarkers associated with sulfur phototrophic bacteria, within the OAE-2 interval would indicate that H<sub>2</sub>S extended at least episodically into the photic zone (Sinninghe Damsté and Köster, 1998; Kuypers et al., 2002; Pancost et al., 2004; Sinninghe Damsté et al., 2008). By compiling and comparing the geochemical data ( $\delta^{15}N_{total}$ ,  $C_{org}$ , trace metal concentrations) obtained as part of this study and from previous reports (Kuypers et al., 2002; Kuypers et al., 2004; Forster et al., 2007; van Helmond et al., 2014a; Westermann et al., 2014;

Dickson et al., 2016) and unpublished data from H-J Brumsack for selected elements (Fe, Mn, P, Cu, Ni, Co, Zr), we propose below to bring further details in the oxygenation evolution of the DSDP site 367.

In the core 19, the EI/Al record is only marked by a peak value at 648.0 m for some elements (V, Zn, Cd, Cu, U), associated to the first noticeable peak of  $C_{org}$  (29.3%), low values of  $\delta^{15}N_{total}$  (−1.8‰) but without perturbation of  $\delta^{13}C_{org}$  signal (Figures 4,5). All of these elements being redox-sensitive, it is likely that this short level of increasing OM burial, recorded few meter before the onset of the OAE-2, was associated to a short-term interval of O<sub>2</sub>-depleted conditions. The peak of 2-methylhopanoid index, used as a marker of cyanobacterial oxygenic photosynthesis (Summons et al., 1999) recorded at 647.95 m in Kuypers et al. (2004) and the absence of isorenieratane, a biomarker of green sulfur cyanobacteria (Kuypers et al., 2002) argue for a well oxygenated photic zone. The water column extension of O<sub>2</sub>-depleted conditions during this interval was probably limited, close to the sediment/water interface. The use of redox ratios, such as U/Th and V/Cr can further constraints the oxygenation level. Based on the dysoxic/anoxic thresholds (1.25 for U/Th, 4.25 for V/Cr), defined by Jones and Manning (1994), these ratios indicate anoxic conditions (Figure 8). Unfortunately, due to poor resolution of sampling around 648.0 m, the lower and upper limits of this interval cannot be precisely defined. Except for this short-term interval, the rest of the core 19 corresponds to dysoxic conditions.

In the core 18, the concentrations of O<sub>2</sub>-sensitive elements (Mo, U, V, Zn, Ni) exhibit fluctuating values within the interval depth corresponding to the OAE-2 (642.0–636.5 m). The base of the OAE-2 (642.0–640.3 m), corresponding to the onset of  $\delta^{13}C$  excursion, and the PCE-1-PCE-2 interval, is characterized by a progressive and noticeable increase in EI/Al ratio for most of the RSTE (e.g., V, U, Ni) with peak value interval recorded around 640.5 m (Figure 4). Similar evolutions are observed for the redox V/Cr and U/Th ratios (Figure 8). The coeval increase of TOC values and most of the RSTE, associated with low values of  $\delta^{15}N_{total}$  (mainly < −1.5‰), clearly indicate the onset of



anoxic to euxinic conditions in the water column (**Figures 2,4**). The extent of O<sub>2</sub>-depleted conditions is supported by cyanobacterial biomarkers (Kuypers et al., 2002). In this interval (642.0–640.35 m), the punctual occurrence of isorenieratane, associated with highest values of P, Cd and Cu (**Figure 5**) argue for an euxinic photic zone, which could be the result of an increase of O<sub>2</sub> demands by the phytoplankton associated with a rise of the chemocline to shallower depths (Kuypers et al., 2002).

This 1.5 m thick interval is followed by a 55 cm thick interval (640.35–639.80 m), corresponding to the PCE-3, that is underlined by an important drop of most of the RSTE (Mo, U, V, and Zn) for both concentrations and El/Al ratios, coeval with a decrease of TOC values of ~20% and an increasing trend of  $\delta^{15}\text{N}_{\text{total}}$  values up to -1.2‰ (**Figures 2,4**). A similar organic-poor interval, characterized by low trace metal concentrations, was previously recorded in proto-North Atlantic deep sites: 1276 and 603 (van Helmond et al., 2014a) but never recognized at

DSDP site 367. This short interval was interpreted at ODP sites 1276 and 603 as a temporary reoxygenation event of the bottom waters as a consequence of the PCE (van Helmond et al., 2014a). At the DSDP site 367, this interval (640.35–639.80 m) strictly correspond to the stratigraphic level where the lowest values of TEX<sub>86</sub> were recorded by Forster et al. (2007) arguing for a cooling of sea surface temperature episode and where a decrease of isorenieratane concentration was observed at 640.11 m in Kuypers et al. (2002). In this deeper site, the PCE thus likely triggered a transient decrease in concentration of dissolved H<sub>2</sub>S in the photic zone and in bottom-water as well. The PCE would thus be associated to a short-term return toward non-euxinic conditions. This perturbation of redox conditions may have altered partially or totally the conversion of Mo, V, and Zn to thiomolybdates, oxides (V<sub>2</sub>O<sub>3</sub> and V(OH)<sub>3</sub>) and sulfides (ZnS), respectively (Tribovillard et al., 2006) and can account for noticeable decrease of El/Al ratio observed for most of the RSTE during this interval. As an alternative to redox



perturbation, enhanced drawdown of seawater trace metal reservoir has been suggested to explain the sizeable decrease of  $O_2/H_2S$  sensitive elements, as documented for two deep ODP sites (1258 and 1260) located in the south-western part of the Central Atlantic at Demerara Rise (Hetzl et al., 2009). For these two sites, the decline of elements concentrations is observed during the entire OAE-2, whereas for the DSDP site 367, this decline is observed only at the end of the P-CIE (for few elements, as Zn, Cu, and Cd continuing in the plateau interval). Most  $O_2/H_2S$  sensitive elements show either a slight enrichment in the plateau interval (e.g. Mo and U) or noticeable enrichment (e.g. V, Ni, and Fe) with the highest value recorded within the plateau interval at 638.1 m (Figures 4, 6). The contrasted behavior of these elements between the DSDP site 367 (Cape Verde) and the ODP sites 1258–1260 (Demerara Rise) argue for a transient decrease in concentration of dissolved  $H_2S$ , associated to the PCE rather than for a drawdown of seawater trace metal reservoir at a global or regional scale. This transient episode of reoxygenation indeed likely replenish trace metals (Jenkyns et al., 2017). This inference is strengthened by the evolution of the  $C_{org}/P_{total}$  ratio and the  $\delta^{15}N_{total}$  signal (Figures 2,3), which show respectively extremely high values ( $>1,000$ ) and low values ( $<-1.6\%$ ) within the plateau interval (this study) and by the high concentration of isorenieratane ( $>50$  mg/g TOC) and high percentage of 2-methylhopanoid ( $>15\%$ ; Kuypers et al., 2004). All the geochemical data suggest that after a short-term episode of  $H_2S$  depletion during the PCE, the water column returns to anoxic-euxinic conditions during the plateau interval. Under these conditions, remobilization and regeneration of some elements like P (phosphate or organic phosphorus) and Ba (barite), during OM remineralization by sulfate reducing bacteria may occur (Van Capellen and Ingall, 1994; Krall et al., 2010). In contrast, in the presence of  $H_2S$  some other elements may form insoluble sulfide phase (CuS,  $CuS_2$ , CdS) or may be incorporated as solid solution (ZnS, NiS, CoS) in pyrite (FeS) (Huerta-Diaz and Morse, 1992). The absence of noticeable enrichment of Cu and Cd compared to those observed for Ni, Co and Fe suggests a preferential co-precipitation with FeS.

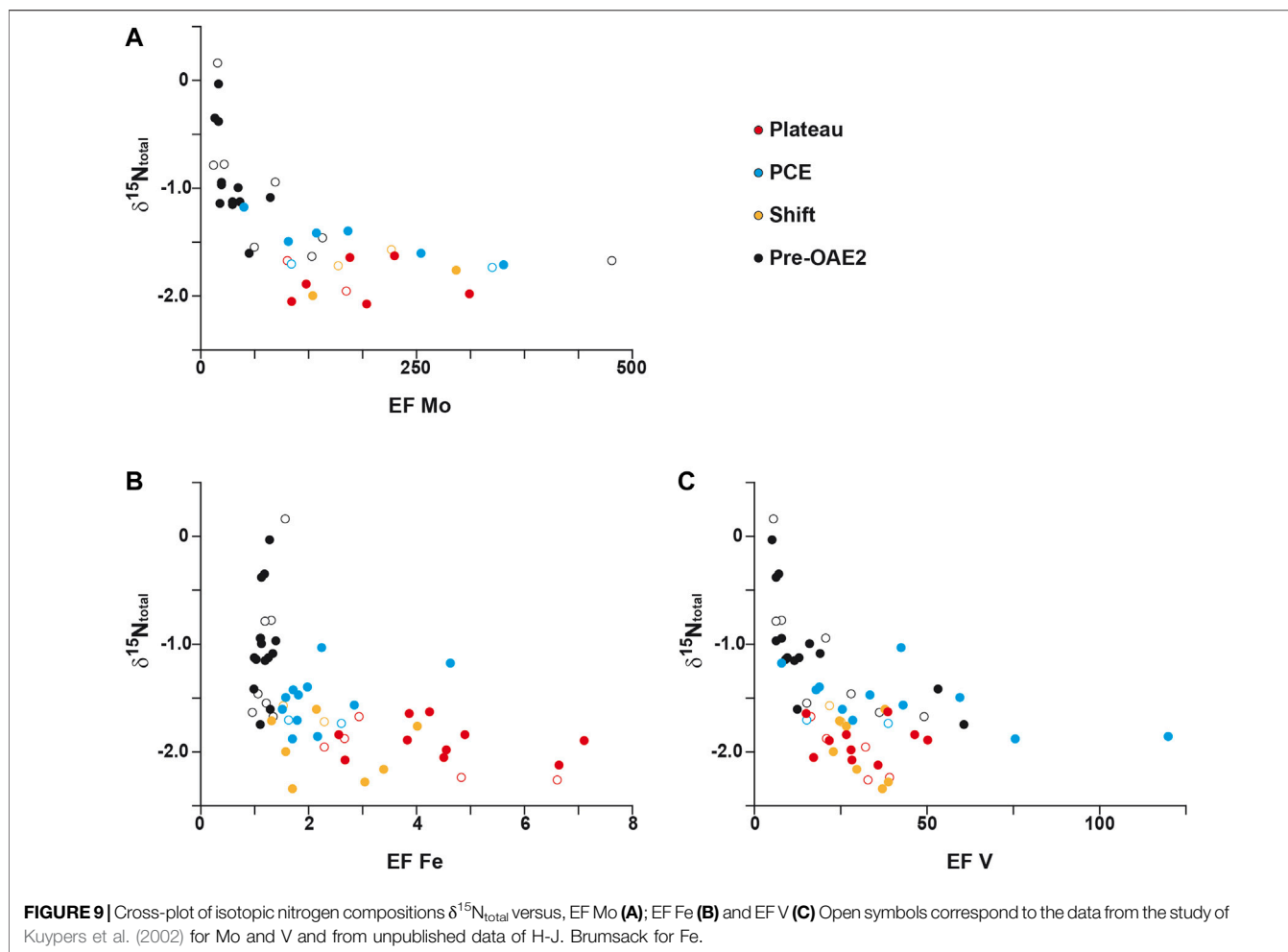
Since the work of Algeo and Lyons (2006) on the covariations of TOC and Mo concentration in modern euxinic basins (i.e., Black Sea, Cariaco Basin), the Mo/TOC ratio is considered as a reliable proxy to estimate intensity of restriction of water mass in silled basins and renewal time of the deep-water mass. By compiling all the Mo/TOC data for the DSDP site 367 (Kuypers et al., 2002; Westermann et al., 2014; Dickson et al., 2016; this study), an abrupt decrease of this ratio is clearly evidence from 440.5 m, with values mainly lower than 2.25 up to 636.5 m depth (Figure 8). This protracted shift toward lower values reflects a decline of Mo concentrations (mainly  $<100$  ppm), associated to an increase of OM preservation (with TOC values  $>25\%$ ) recorded in samples from the top of the P-CIE (P-CIE-3) and the plateau intervals of the DSDP site 367. In details, the lowest values of Mo/TOC ratio are mainly recorded in the 1-m thick interval (640.5–639.5 m) corresponding to the PCE. This event, which lasted 40–65 kyr (O'Connor et al., 2020), record a reoxygenation of deep and shallow water domain and a cooling event (drop in sea-surface temperature of  $\sim 2.5$ – $5.5^\circ C$ , Forster

et al., 2007) and likely corresponds here to an episode of water-masses renewal. We suggest that during this short-term event, the concentration of  $H_2S$  was too low to convert molybdate anions to particle-reactive thiomolybdates. Accordingly, we suggest that the low Mo/TOC values observed for the Cape Verde sediments during the PCE reflect an anoxic unrestricted environment, associated with dynamic water masses such as upwelling system rather than a restricted silled basin. For the remaining of the sedimentary record of the OAE-2, the Mo/TOC values mainly oscillate from 1 to 10 with an average value around 4.4, close to the regression slope value of 4.1, proposed by van Helmond et al. (2014a) for the deep proto-North Atlantic and the reference value of 4.5 obtained for the Black Sea (Algeo and Lyons, 2006), suggesting a water mass renewal period longer than 500 years.

## General Framework of Nitrogen Isotope Signals Interpretations During the Oceanic Anoxic Event 2

Widespread changes of oxygen availability in the water column during the establishment of the OAE-2 have sensibly affected the cycle of N, which is considered as the main limiting nutrient with P and Fe. In general, extended anoxic conditions lead to an enhanced nitrogen loss through denitrification and ammonium oxidation processes, in which case an anoxic bottom part of the water column becomes  $NH_4^+$ -rich and  $N_2$ -fixation could overcome nitrate limitation to support biological productivity. Isotopic fractionation associated with atmospheric  $N_2$ -fixation by diazotrophs being low, the  $\delta^{15}N_{total}$  values could tend towards  $\sim 0\%$ .

Changes of bioavailable dissolved nitrogen  $\delta^{15}N_{total}$  over geological times mainly reflect the balance between the dominant nitrogen metabolic pathways regulating the nitrogen cycle alongside the water column structure (Sigman et al., 2009; Thomazo and Papineau, 2013; Ader et al., 2016; Stüeken et al., 2016). The Cretaceous Period is overall characterized by an elevated sea level and a warm climate, both affecting the water column stratification and dynamics and thus impacting the evolution of the sedimentary  $\delta^{15}N_{total}$ . Indeed, sea level variation is known to potentially change the locus of denitrification in oceanic settings (Deutsch et al., 2004). High sea level appears to enhance organic carbon burial in highly productive continental shelves by favouring sedimentary denitrification (Algeo et al., 2014). However, this highlighted correlation between sea level elevation and sedimentary  $\delta^{15}N_{total}$  evolution through Greenhouse/Icehouse period might require to be nuanced concerning the OAE-2. Indeed, during this widespread anoxic event, numerous continental shelf environments appear to also evidence water column anoxic condition and hence active water column denitrification. It was also suggested that during the mid-Cretaceous Greenhouse period, high sea levels and the continental configuration favoured the formation by evaporation of warm and saline water masses in low latitude, inducing the formation of deep-water masses (Brass et al., 1982; Friedrich et al., 2006). This process could have favoured water column mixing and thus facilitated the input of  $NH_4^+$ -rich water masses to the surface. It probably occurred during the onset of the OAE-2 but was interrupted or at least highly reduced during the PCE, due to reduced evaporation and drier climate.

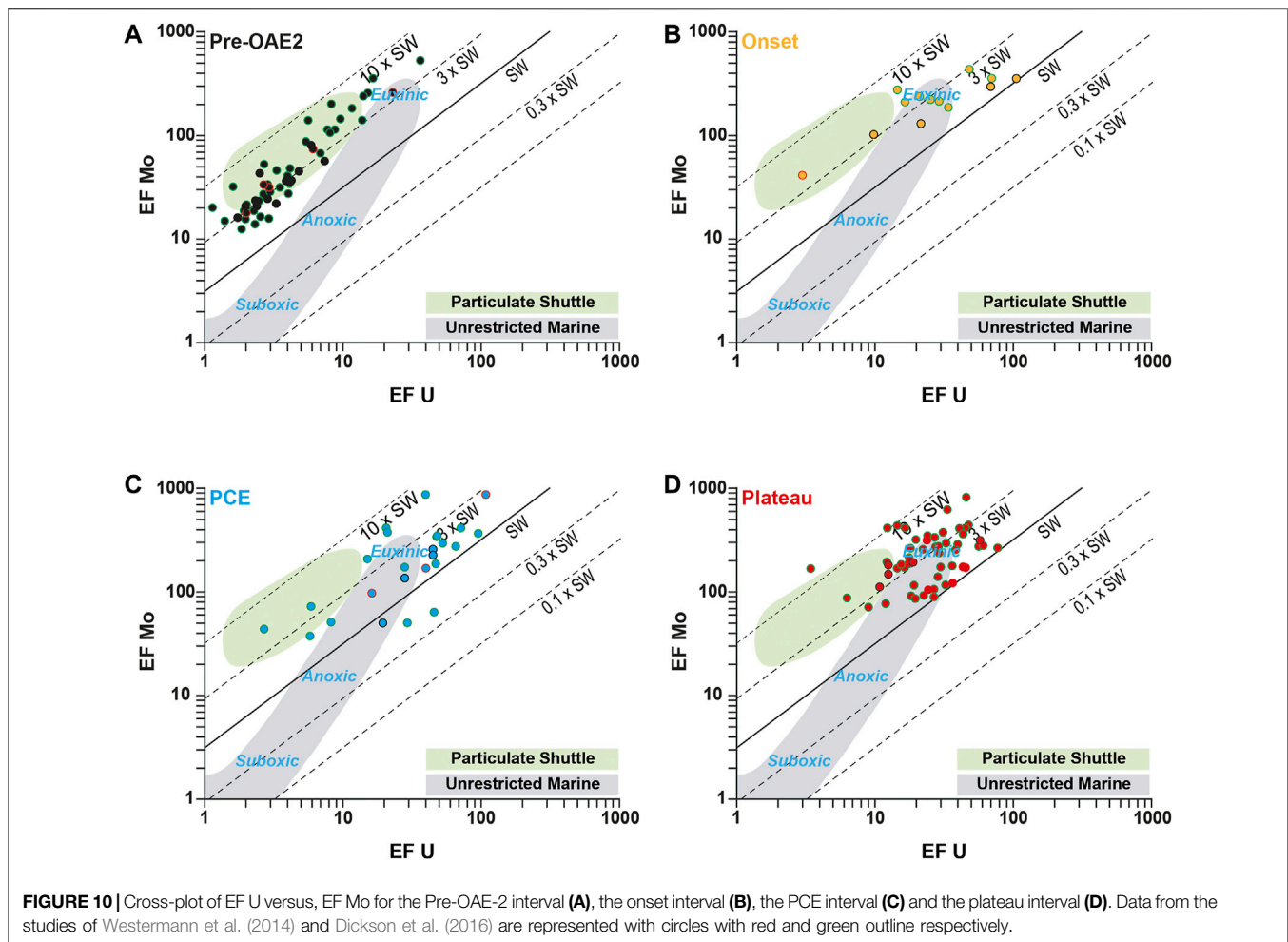


At the DSDP site 367, the low and negative  $\delta^{15}\text{N}_{\text{total}}$  values (0 to  $-2.3\text{‰}$ ) confirm the data previously obtained by Kuypers et al. (2004), and are consistent with the mainly negative  $\delta^{15}\text{N}_{\text{total}}$  values reported in proto-North and Central Atlantic sites recording the OAE-2 (e.g., ODP sites 1260; 1261 and 1276), with  $\delta^{15}\text{N}_{\text{total}}$  mostly comprised between  $-4$  and  $2\text{‰}$  (Jenkyns et al., 2007; Junium and Arthur, 2007; Ruvalcaba Baroni et al., 2015). These isotopic values associated with elevated 2-methylhopanoid ratio at the DSDP site 367 have been initially attributed to a significant uptake of  $\text{N}_2$  by diazotrophs (Kuypers et al., 2002). Such low  $\delta^{15}\text{N}_{\text{total}}$  values are, however, significantly lower than  $\delta^{15}\text{N}_{\text{total}}$  values observed in modern anoxic basins (e.g. Black Sea, Cariaco Basin) in which  $\text{N}_2$ -fixation is known to be significant (Fry et al., 1991; Thunell et al., 2004). To explain these negative  $\delta^{15}\text{N}_{\text{total}}$  values, it was suggested that upwelling of anoxic and ammonium-rich deep waters have supported biological productivity by providing dissolved fixed-nitrogen to primary producers (Higgins et al., 2012).

During the OAE-2, deep oceanic settings, as the DSDP site 367, can indeed build up a large reservoir of  $\text{NH}_4^+$ , which can be the main  $\text{N}$  source for primary production (ammonia ocean scenario of Higgins et al., 2012). In such scenario, a combination of denitrification and anammox reactions at the

chemocline quantitatively consumes the nitrate and nitrite reservoir, the primary productivity being supported by advection of  $^{15}\text{N}$ -depleted  $\text{NH}_4^+$ , as well as other nutrient elements like  $\text{PO}_4^{3-}$ , from deep water up to the photic zone, especially during chemocline upward excursions. The  $^{15}\text{N}$ -depleted  $\text{NH}_4^+$  can be consumed through ammonium assimilation and ammonium oxidation (i.e., nitrification), which are both associated to a sizeable isotopic fractionation that generate a  $^{15}\text{N}$ -depleted product and  $^{15}\text{N}$ -enriched residual  $\text{NH}_4^+$  reservoir. If the fractionation associated with ammonium assimilation outcompetes the isotopic enrichment caused by the combination of anammox/denitrification/nitrification processes, the biomass remains isotopically negative.

Alternative nitrogenases to  $\text{N}_2$ -fixation using Fe and V rather than Mo as enzymatic co-factor was also proposed to explain  $\delta^{15}\text{N}_{\text{total}}$  values lower than  $-2\text{‰}$  recorded during OAE-2 in the proto-North and Central Atlantic sites (Zhang et al., 2014). In this scenario, Mo is replaced in the active site of the metalloenzyme by Fe or V in response of the global oceanic drawdown of trace metals (especially Mo). These alternative nitrogenases can be expressed either by cyanobacteria in the photic zone or by anoxygenic phototrophs and would be favored during period



of increase in the Fe/Mo ratio possibly linked to enhance hydrothermal activity and Mo scavenging. However, no clear difference is observed between Mo and Fe in a scatterplot with  $\delta^{15}\text{N}_{\text{total}}$  values (Figure 9) in our dataset. Both elements are characterized by a nonlinear negative correlation with  $\delta^{15}\text{N}_{\text{total}}$ . Moreover, the alternative nitrogenase hypothesis implied a large  $\delta^{15}\text{N}$  fractionation down to  $-7\%$ , while the minimum value recorded at DSDP site 367 is  $-2.3\%$ . We therefore suggest that the contribution of  $\text{N}_2$ -fixation through an alternative nitrogenase while possible could only represent a small proportion of  $\delta^{15}\text{N}_{\text{total}}$  signal, due to both 1) mass balance considerations and 2) the reported high abundance of eukaryotic biomass at Demerara Rise, in a similar paleogeographical context and with equivalent  $\delta^{15}\text{N}$  values during OAE-2 (Higgins et al., 2012).

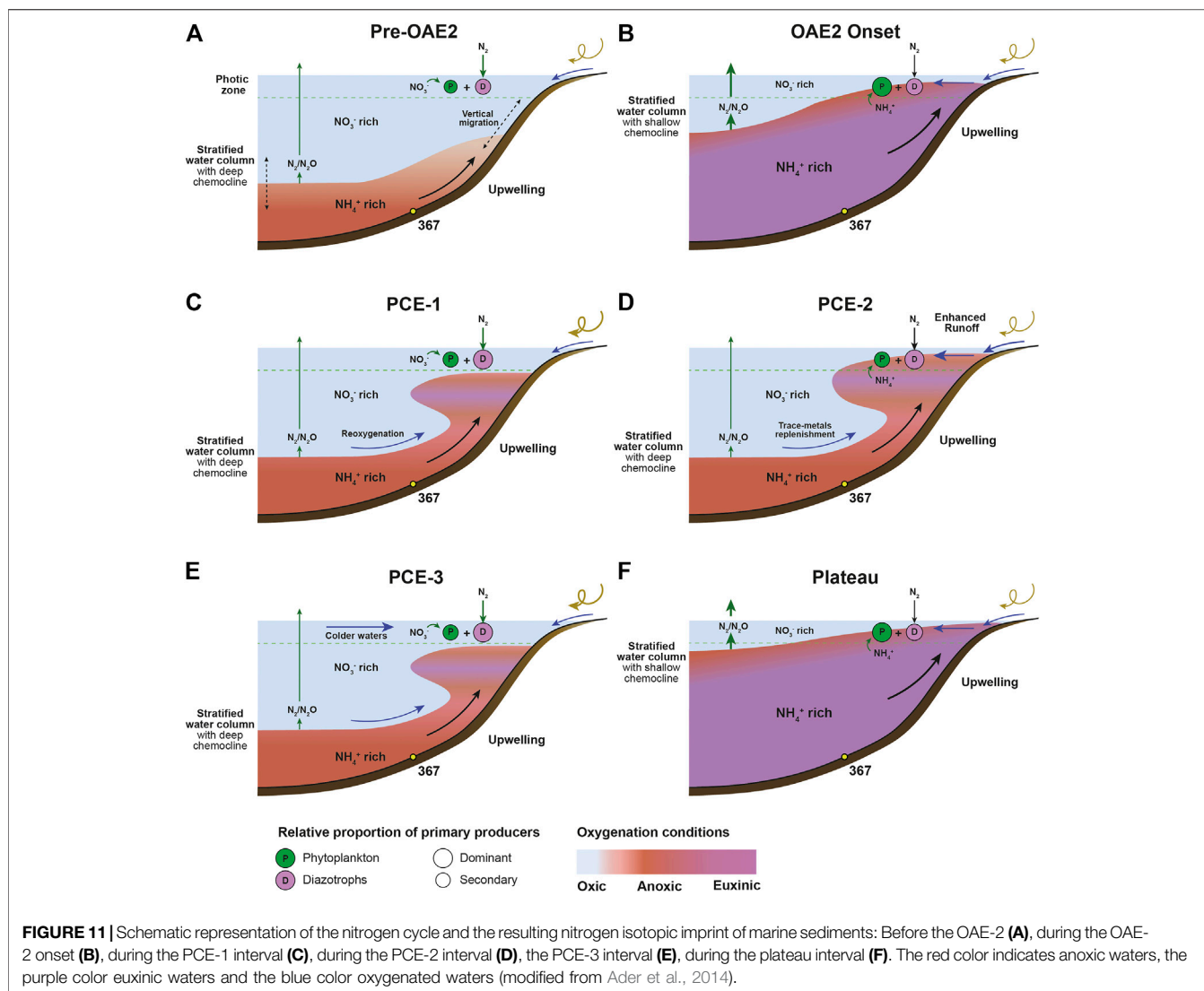
Our  $\delta^{15}\text{N}_{\text{total}}$  data, at the first order, seem to agree with the proposed combination of  $^{15}\text{N}$ -depleted ammonium assimilation and  $\text{N}_2$ -fixation to explain the low and negative isotopic values observed. Moreover, our high-resolution  $\delta^{15}\text{N}_{\text{total}}$  analysis revealed significant short-term  $\delta^{15}\text{N}_{\text{total}}$  variations related to physical and chemical changes associated to both the OAE-2 and the PCE which are discussed below.

## High Resolution Nitrogen Isotopes Variations Across Oceanic Anoxic Event 2 and Plenius Cold Event Records at Cape Verde

### Pre-Oceanic Anoxic Event Nitrogen Cycle

The specificity of the Central Atlantic is to show evidences of deoxygenated conditions before the OAE-2. In the Cape Verde basin, this pre-OAE deoxygenation is expressed by continuous high amount of OM, detectable authigenic enrichments ( $3 < \text{EF} < 10$ ) of most RSTE and evidences of an active phosphorus regeneration. Besides, high Mo enrichments compared to U suggest an active “Particulate shuttle” effect in water column (Figure 10), as reported for modern semi-enclosed basins (Algeo and Tribovillard, 2009; Tribovillard et al., 2012), hence suggesting that a strong and deep chemocline discriminates a well oxygenated upper water column from anoxic bottom waters. The redox conditions were, however, not stable during this Pre-OAE time, and periods of stronger deoxygenation stand out such as within the section 3 of the core 19.

During this pre-OAE interval, constantly negative  $\delta^{15}\text{N}$  values ( $-1.2$  to  $0\%$ ) indicate that  $\text{N}_2$ -fixation outcompetes  $\text{NO}_3^-$



limitation in the photic zone (Figure 11). Within the framework of a stratified water column, quantitative N loss due to the combination of nitrification, heterotrophic denitrification and anammox occur at the chemocline while  $\text{NH}_4^+$  could accumulate in the deeper basin.

While being presumably stratified before the OAE-2, oceanographic models (Trabucho Alexandre et al., 2010; Topper et al., 2011) proposed that during the mid-Cretaceous time the Southeastern part of the Central Atlantic basin was characterized by the presence of upwelling currents along margins bringing  $\text{NH}_4^+$  rich waters from the deep ocean toward the surface, transiently reaching the photic zone. Anoxia in the photic zone preceding the OAE was previously proposed to account for punctual isorenieratane occurrences (Kuypers et al., 2002). In addition to the long term stratification of the Cape Verde basin, delivery of  $^{15}\text{N}$ -depleted  $\text{NH}_4^+$  in the photic zone from more proximal areas may have been assimilated by the phytoplankton and consequently participate to the lowest  $\delta^{15}\text{N}$  values observed in the section 3 of the core 19 (down to  $-1.75\%$ ). Other possible mechanisms of deep-

water advection into the surface include eddy-circulation, which may have been particularly relevant of the mid-Cretaceous ice-free climate regime (Hay, 2008).

### Oceanic Anoxic Event 2 Nitrogen Cycle

At DSDP site 367, the first  $\delta^{13}\text{C}$  buildup and the plateau interval within the OAE-2 are characterized by an intensification of the deoxygenation as demonstrated by the substantial authigenic enrichment of the RSTE (e.g., U, Ni, V) leading to euxinic conditions in the basin. Large proportions of sulfide in the water column are also evidenced by exceptionally intense P recycling rate, marked by high  $C_{\text{org}}/P_{\text{total}}$  values (this study) and by a rapid positive excursion of the  $\delta^{98/95}\text{Mo}$  (Westermann et al., 2014; Dickson et al., 2016), towards the typical seawater composition. The shallowing of the chemocline, and hence the invasion of the euxinic conditions from the bottom waters to the photic zone, was also demonstrated by the large concentrations of isorenieratane measured along the OAE-2 and mostly during the plateau interval (Kuypers et al., 2002).



At DSDP site 367, the Mo vs. U enrichments during the onset of the OAE-2 and the plateau intervals are mostly located in the “Euxinic” zone or even higher (Figure 10). Thus, the EF Mo/EF U values decrease during the two episodes of extreme deoxygenation approaching the values of today’s seawater (~7.7). Significantly, while the plateau interval is the period characterized by the most intense and the most prolonged deoxygenated conditions of the OAE-2, enrichments in some RSTE as Mo, U or V are lower in this interval than during PCE, conversely to Fe. This observation, combined with low Mo/TOC values, suggests a drawdown of these elements in the water-column due to their scavenging in the sediments at the basin scale.

In the proto-North and Central Atlantic sites, negative  $\delta^{15}\text{N}_{\text{total}}$  values during the OAE-2 has been largely reported in every part of the ocean (Kuypers et al., 2004; Junium and Arthur, 2007; Higgins et al., 2012; Ruvalcaba Baroni et al., 2015). This negative signal is consistent with a combination of both  $\text{N}_2$ -fixation and  $\text{NH}_4^+$  partial assimilation processes in the N export production. While both  $\text{N}_2$ -fixation and  $\text{NH}_4^+$  assimilation were important in the nitrogen exported production, a general lowering of the  $\delta^{15}\text{N}_{\text{total}}$  value from North to South suggests that the  $\text{NH}_4^+$  assimilation was particularly significant in the southern part (Ruvalcaba Baroni et al., 2015; Naafs et al., 2019) and could have been dominant, as evidenced by Higgins et al. (2012). The high  $\text{C}_{\text{org}}/\text{N}_{\text{total}}$  ratio, observed in the DSDP 367 site indicates an intense biological removal of amino groups from the OM in the sediments, releasing  $\text{NH}_4^+$ . The diffused  $\text{NH}_4^+$  from the sediments would have further supplied a water column ammonium reservoir.

At DSDP site 367, the evolution of the  $\delta^{15}\text{N}_{\text{total}}$  is fully consistent with the convecting redox-stratified ocean model proposed by Ader et al., 2014; Ader et al., 2016) where  $\text{NH}_4^+$  invades the entire basin and  $\text{NO}_3^-$  reservoir is substantially reduced and limited in the photic zone far away from the coastal area (Figure 11). The limited  $\delta^{15}\text{N}_{\text{total}}$  fluctuations during the plateau interval would therefore represent variations in the relative proportions between the eukaryotic and the denitrifying biomasses, which would be controlled by the position of the chemocline through the lower limit of the photic zone. The large variations in the Fe enrichments are coherent with fluctuations of the  $\text{H}_2\text{S}$  inventory of the water-column chemocline. Redox fluctuations with a similar pace were previously evidenced by oscillating  $\delta^{98/95}\text{Mo}$ , that were interpreted as the expression of orbital cycles controlling the continental-weathering and the delivery of nutrient in the basin (Dickson et al., 2016), suggesting a climate influence on oxygenation conditions and nitrogen cycle. Comparable variations in Fe chemistry,  $\text{C}_{\text{org}}/\text{P}_{\text{total}}$  ratio (Poulton et al., 2015) and  $\delta^{98/95}\text{Mo}$  variations (Goldberg et al., 2016) with those measured in the Cape Verde Basin were evidenced along the same continental margin in the Tarfaya Basin (Offshore Morocco), in a shelf setting. This observation highlights that the redox fluctuations described in the deep Cape Verde Basin are consistent with shallower settings and confirm that they are constrained by the regional redox structure of the entire southern proto-North Atlantic domain. Besides, continuous  $\text{O}_2$ -depleted conditions at intermediate bathymetry (>1,000 m for the deepest site) from pre-to post-OAE-2 at Demerara Rise (Hetzl et al., 2009) suggest that an expanded Oxygen-Minimum Zone impinged the southern part of the proto-

North Atlantic, and we suggest that upwelling currents were active through the Cenomanian-Turonian interval in this region.

### Nitrogen Cycle During the Plenus Cold Event

The high resolution of the  $\delta^{15}\text{N}_{\text{total}}$  signal measured along the section not only allowed to distinguish the PCE during the OAE-2, but also to highlight large variations characterizing a complex N cycle during this swing in temperature. Indeed, the PCE interval is particularly well underlined by two spikes of heavier  $\delta^{15}\text{N}_{\text{total}}$  values recorded during the PCE-1 and PCE-3. This period was also previously associated with a deepening of the chemocline based on a drop in the  $\delta^{98/95}\text{Mo}$  values (Dickson et al., 2016). However, still high enrichments in Mo, and in a lesser degree in U, argue for persistent anoxic to euxinic deep waters (Figure 10). Active upwelling currents bringing nutrients rich waters to the surface, hence maintaining a high primary production and  $\text{C}_{\text{org}}$  export to the sediments may have promoted the formation of an oxygen rich intermediate water mass along the Cape Verde basin margin.

We suggest that PCE-1 represents a period of better-ventilated intermediate waters. The rapid and large increase in  $\delta^{15}\text{N}_{\text{total}}$  within the PCE-1 (+1.3‰) is consistent with a switch in the nitrogen cycle with higher ratio of nitrate vs ammonium assimilation the former expanding due to upwelling of oxygenated water masses (Figure 11). In both cases however,  $\text{N}_2$ -fixation likely represents the main source of N for primary producers,  $\delta^{15}\text{N}_{\text{total}}$  remaining close to 0‰ value, as expected in stratified settings (Figure 11).

The PCE-2 is associated with lower  $\delta^{15}\text{N}_{\text{total}}$  values (~-1.8‰) and many trace metal (Cd, Cu, Ni, V, Zn) enrichments (Figures 3–5). Such enrichments in an overall period of reoxygenation has previously been reported in the Western Interior Seaway (Eldrett et al., 2014) or in the English Chalk (Jenkyns et al., 2017), and were either interpreted as the advent of waters rich in hydrothermally-derived elements or by basin-scale re-oxidation of previously deposited organic- and sulfide-rich sediments. Oxygenated water masses may have been restricted “in sandwich” between two ammonium rich and nitrate poor water masses and the overall nitrogen cycle back to an isotopic signal of  $\text{N}_2$ -fixation and  $\text{NH}_4^+$  partial assimilation state on proximal margin.

The second peak of heavier  $\delta^{15}\text{N}_{\text{total}}$  values in the PCE-3 is accompanied with both a drop in sea-surface temperature (Forster et al., 2007) and a reoxygenation of the basin as demonstrated by the lowest trace metal enrichments. This transient cooling and reoxygenation may have cause a deepening of the chemocline and increase in the contribution of nitrate to the nitrogen isotope sedimentary signal. Compared to long-term secular variations observed during greenhouse-icehouse periods (Algeo et al., 2014), the PCE nitrogen cycling point out to a more complex picture. Indeed, if water column denitrification can expand during the PCE and imprint the geochemical sedimentary record due to an increasing contribution of cycled nitrate to the biomass, we suggest that associated changes in the  $\delta^{15}\text{N}_{\text{total}}$  signal are primarily controlled by the ratio of bioavailable ammonium to nitrate rather than a change in the locus (sedimentary vs water column) of denitrification. This inference is supported by recent results of Earth System model which demonstrates that during the OAE-2 fundamental transitions in the species of nitrogen

dominating the fixed-N inventory, from nitrate to ammonium across deoxygenation, are anticipated (Naafs et al., 2019).

## CONCLUSION

By combining newly generated and existing geochemical data from the DSDP site 367, our integrated study:

- confirms the burial of organic matter, dominantly marine in origin, associated to a positive carbon isotopic excursion of ~6.0‰. For this isotopic excursion, a detailed sequencing of  $\delta^{13}\text{C}$  evolution has been proposed and a new subdivision within the Plenus carbon isotopic excursion in three sub-intervals (PCE-1, PCE-2, and PCE-3) is suggested.

- highlights the fluctuations of oxygenation in the water column especially during the Plenus carbon isotopic excursion for one the deepest site in the Central Atlantic. After a period of stability in concentration of redox sensitive trace elements and high  $\delta^{15}\text{N}_{\text{total}}$  values (>−1.2‰), characterized by dysoxic to anoxic conditions before the OAE-2, the onset of this event, marked by noticeable enrichment of these elements and the lowest  $\delta^{15}\text{N}_{\text{total}}$  values (<−2.0‰), is associated to euxinic conditions in bottom water. Within the OAE-2, the Plenus carbon isotopic excursion is associated to short-term  $\text{O}_2/\text{H}_2\text{S}$  fluctuations and three settings are distinguished. The PCE-1, characterized by decreasing trend of  $\delta^{15}\text{N}_{\text{total}}$  values and contrasted record of redox sensitive trace elements, would correspond to a period of better-ventilated intermediate waters. The PCE-2, marked by noticeable enrichment of these elements and the lower  $\delta^{15}\text{N}_{\text{total}}$  values (~−2.0‰), is characterized by water column  $\text{O}_2$ -depleted conditions, associated to potential hydrothermal enrichments. The PCE-3, marked by noticeable decreasing trend of both  $\delta^{15}\text{N}_{\text{total}}$  values and redox sensitive trace elements, is interpreted as an interval of reoxygenation of water column, probably linked to input of cooler and oxygenated water from high latitudes. Lastly, the plateau interval is marked by the invasion of the euxinic conditions from the bottom waters up to the photic zone.

- discusses for the first time the impact of the Plenus Cold Event on the nitrogen cycle for this site and a model for the nitrogen cycle and the resulting nitrogen isotopic imprint of marine sediments is proposed. Before the OAE-2, a stratified water column model and a deep and strong chemocline, prevailed in  $\text{NH}_4^+$ -rich bottom water. The onset of the OAE-2 is characterized by the development in the water column of euxinic  $\text{NH}_4^+$  rich water masses, and a restriction of the  $\text{NO}_3^-$  reservoir to the photic zone. These nitrogen cycle settings changed during the short-term climatic variations associated with the Plenus

Cold Event. During cooling, a reoxygenation phase of the intermediate water due to active upwelling currents and accompanied by a deepening of a sulfide-rich chemocline temporally reshaped both the carbon and nitrogen cycles. These changes are remarkably well expressed in the nitrogen isotope record with swings in the  $\delta^{15}\text{N}_{\text{total}}$  values, interpreted here as a tracer of ammonium to nitrate bioavailable inventory.

## DATA AVAILABILITY STATEMENT

The original contributions presented in the study are included in the article/**Supplementary Materials**, further inquiries can be directed to the corresponding author/s.

## AUTHOR CONTRIBUTIONS

PC performed the isotopic geochemical analysis and FB performed the organic geochemical analysis. LR, PC, FB, CT, and JD contributed to the interpretation of the results. LR organized the database and wrote the first draft of the manuscript. LR, PC, JD, and CT wrote sections of the manuscript. All authors contributed to manuscript revision, read, and approved the submitted version.

## ACKNOWLEDGMENTS

We would like to thank Florence Savignac for her analytical assistance for Rock-Eval analysis, Marie-Jeanne Milloux for organic isotope measurements and Alexandre Lethiers for illustration support. Hans-Jürgen Brumsack is kindly thanked for sharing unpublished data for selected major and trace elements. We also thank J-C M-S and Y-U Z for providing constructive comments. This research used samples provided by the International Ocean Discovery Program. This study was funded by the project Anox-Sea ANR-12-BS06-0011 coordinated by EP. Data from this study can be found in the supplementary data file.

## SUPPLEMENTARY MATERIAL

The Supplementary Material for this article can be found online at: <https://www.frontiersin.org/articles/10.3389/feart.2021.703282/full#supplementary-material>

## REFERENCES

- Ader, M., Sansjofre, P., Halverson, G. P., Busigny, V., Trindade, R. I. F., Kunzmann, M., et al. (2014). Ocean Redox Structure across the Late Neoproterozoic Oxygenation Event: a Nitrogen Isotope Perspective. *Earth Planet. Sci. Lett.* 396, 1–13. doi:10.1016/j.epsl.2014.03.042
- Ader, M., Thomazo, C., Sansjofre, P., Busigny, V., Papineau, D., Laffont, R., et al. (2016). Interpretation of the Nitrogen Isotopic Composition of Precambrian Sedimentary Rocks: Assumptions and Perspectives. *Chem. Geology* 429, 93–110. doi:10.1016/j.chemgeo.2016.02.010
- Algeo, T. J., and Lyons, T. W. (2006). Mo-Total Organic Carbon Covariation in Modern Anoxic marine Environments: Implications for Analysis of Paleoredox and Paleohydrographic Conditions. *Paleoceanography* 21, PA1016. doi:10.1029/PA00111210.1029/2004pa001112
- Algeo, T. J., and Tribovillard, N. (2009). Environmental Analysis of Paleocyanographic Systems Based on Molybdenum-Uranium Covariation. *Chem. Geology* 268, 211–225. doi:10.1016/j.chemgeo.2009.09.001
- Algeo, T. J., Meyers, P. A., Robinson, R. S., Rowe, H., and Jiang, G. Q. (2014). Icehouse-greenhouse Variations in marine Denitrification. *Biogeosciences* 11 (4), 1273–1295. doi:10.5194/bg-11-1273-2014

- Arthur, M. A., Dean, W. E., and Pratt, L. M. (1988). Geochemical and Climatic Effects of Increased marine Organic Carbon Burial at the Cenomanian/Turonian Boundary. *Nature* 335, 714–717. doi:10.1038/335714a0
- Barclay, R. S., McElwain, J. C., and Sageman, B. B. (2010). Carbon Sequestration Activated by a Volcanic CO<sub>2</sub> Pulse during Ocean Anoxic Event 2. *Nat. Geosci.* 3 (3), 205–208. doi:10.1038/ngeo757
- Behar, F., Beaumont, V., and De B. Penteado, H. L. (2001). Rock-Eval 6 Technology: Performances and Developments. *Oil Gas Sci. Technol. - Rev. IFP* 56, 111–134. doi:10.2516/ogst:2001013
- Blättler, C. L., Jenkyns, H. C., Reynard, L. M., and Henderson, G. M. (2011). Significant Increases in Global Weathering during Oceanic Anoxic Events 1a and 2 Indicated by Calcium Isotopes. *Earth Planet. Sci. Lett.* 309 (1–2), 77–88. doi:10.1016/j.epsl.2011.06.029
- Bowman, A. R., and Bralower, T. J. (2005). Paleoceanographic Significance of High-Resolution Carbon Isotope Records across the Cenomanian-Turonian Boundary in the Western Interior and New Jersey Coastal plain, USA. *Mar. Geology* 217 (3–4), 305–321. doi:10.1016/j.margeo.2005.02.010
- Brandes, J. A., and Devol, A. H. (2002). A Global Marine-Fixed Nitrogen Isotopic Budget: Implications for Holocene Nitrogen Cycling. *Glob. Biogeochem. Cycles* 16 (4), 1120. doi:10.1029/2001GB001856
- Brass, G. W., Southam, J. R., and Peterson, W. H. (1982). Warm saline Bottom Water in the Ancient Ocean. *Nature* 296, 620–623. doi:10.1038/296620a0
- Brumsack, H.-J. (2006). The Trace Metal Content of Recent Organic Carbon-Rich Sediments: Implications for Cretaceous Black Shale Formation. *Palaeogeogr. Palaeoclimatol. Palaeoecol.* 232, 344–361. doi:10.1016/j.palaeo.2005.05.011
- Charbonnier, G., Boulila, S., Spangenberg, J. E., Adatte, T., Föllmi, K. B., and Laskar, J. (2018). Obliquity Pacing of the Hydrological Cycle during the Oceanic Anoxic Event 2. *Earth Planet. Sci. Lett.* 499, 266–277. doi:10.1016/j.epsl.2018.07.029
- Chenet, P.-Y., and Francheteau, J. (1979). “Bathymetric Reconstruction Method : Application to the Central Atlantic Basin between 10°N and 40°N,” in *Deep Sea Drilling Project Initial Report* (Washington, D. C.: U.S. Gov. Print. Off.), 1501–1514. 51, 52, 53, Part 2.
- Clarkson, M. O., Stirling, C. H., Jenkyns, H. C., Dickson, A. J., Porcelli, D., Moy, C. M., et al. (2018). Uranium Isotope Evidence for Two Episodes of Deoxygenation during Oceanic Anoxic Event 2. *Proc. Natl. Acad. Sci. USA* 115 (12), 2918–2923. doi:10.1073/pnas.1715278115
- Danzelle, J., Riquier, L., Baudin, F., Thomazo, C., and Pucéat, E. (2018). Oscillating Redox Conditions in the Vocontian Basin (SE France) during Oceanic Anoxic Event 2 (OAE 2). *Chem. Geology* 493, 136–152. doi:10.1016/j.chemgeo.2018.05.039
- Danzelle, J., Riquier, L., Baudin, F., Thomazo, C., and Pucéat, E. (2020). Nitrogen and Carbon Cycle Perturbations through the Cenomanian-Turonian Oceanic Anoxic Event 2 (~94 Ma) in the Vocontian Basin (SE France). *Palaeogeogr. Palaeoclimatol. Palaeoecol.* 538, 109443. doi:10.1016/j.palaeo.2019.109443
- Deutsch, C., Sigman, D. M., Thunell, R. C., Meckler, A. N., and Haug, G. H. (2004). Isotopic Constraints on Glacial/interglacial Changes in the Oceanic Nitrogen Budget. *Glob. Biogeochem. Cycles* 18. doi:10.1029/2003GB002189
- Dickson, A. J., Jenkyns, H. C., Porcelli, D., van den Boorn, S., and Idiz, E. (2016). Basin-Scale Controls on the Molybdenum-Isotope Composition of Seawater during Oceanic Anoxic Event 2 (Late Cretaceous). *Geochim. Cosmochim. Acta* 178, 291–306. doi:10.1016/j.gca.2015.12.036
- Du Vivier, A. D. C., Selby, D., Condon, D. J., Takashima, R., and Nishi, H. (2015). Pacific 187 Os/188 Os Isotope Chemistry and U-Pb Geochronology: Synchronicity of Global Os Isotope Change Across OAE 2. *Earth Planet. Sci. Lett.* 428, 204–216. doi:10.1016/j.epsl.2015.07.020
- Eldrett, J. S., Minisini, D., and Bergman, S. C. (2014). Decoupling of the Carbon Cycle During Ocean Anoxic Event 2. *Geology* 42 (7), 567–570. doi:10.1130/g35520.1
- Erbacher, J., Mosher, D. C., Malone, M. J., Berti, D., Bice, K. L., Bostock, H., et al. (2004a). “Site 1258,” in *Proc. ODP, Init. Repts.* Editors J. Erbacher, D. C. Mosher, and M. J. Malone (College Station, TX: Ocean Drilling Program), 207, 1–117. doi:10.2973/odp.proc.ir.207.105.2004
- Erbacher, J., Mosher, D. C., Malone, M. J., Berti, D., Bice, K. L., Bostock, H., et al. (2004b). “Site 1260,” in *Proc. ODP, Init. Repts.* Editors J. Erbacher, D. C. Mosher, and M. J. Malone (College Station, TX: Ocean Drilling Program), 207, 1–113. doi:10.2973/odp.proc.ir.207.107.2004
- Erbacher, J., Friedrich, O., Wilson, P. A., Birch, H., and Mutterlose, J. (2005). Stable Organic Carbon Isotope Stratigraphy across Oceanic Anoxic Event 2 of Demerara Rise, Western Tropical Atlantic. *Geochem. Geophys. Geosyst.* 6, Q06010. doi:10.1029/2004GC000850
- Espitalié, J., Deroo, G., and Marquis, F. (1985a). La pyrolyse Rock-Eval et ses applications. Première partie. *Rev. Inst. Fr. Pét.* 40, 563–579. doi:10.2516/ogst:1985035
- Espitalié, J., Deroo, G., and Marquis, F. (1985b). La pyrolyse Rock-Eval et ses applications. Deuxième partie. *Rev. Inst. Fr. Pét.* 40, 755–784. doi:10.2516/ogst:1985045
- Espitalié, J., Deroo, G., and Marquis, F. (1986). La pyrolyse Rock-Eval et ses applications. Troisième partie. *Rev. Inst. Fr. Pét.* 41, 73–89. doi:10.2516/ogst:1986003
- Forster, A., Schouten, S., Moriya, K., Wilson, P. A., and Sinninghe Damste, S. (2007). Tropical Warming and Intermittent Cooling during the Cenomanian/Turonian Oceanic Anoxic Event 2: Sea Surface Temperature Record from the Equatorial Atlantic. *Paleoceanography* 22, 1219. doi:10.1029/PA001349
- Freeman, K. H., and Hayes, J. M. (1992). Fractionation of Carbon Isotopes by Phytoplankton and Estimates of Ancient CO<sub>2</sub> levels. *Glob. Biogeochem. Cycles* 6 (2), 185–198. doi:10.1029/92gb00190
- Friedrich, O., Erbacher, J., and Mutterlose, J. (2006). Paleoenvironmental Changes across the Cenomanian/Turonian Boundary Event (Oceanic Anoxic Event 2) as Indicated by Benthic Foraminifera from the Demerara Rise (ODP Leg 207). *Revue de Micropaléontol.* 49 (3), 121–139. doi:10.1016/j.revmic.2006.04.003
- Fry, B., Jannasch, H. W., Molyneux, S. J., Wirsén, C. O., Muramoto, J. A., and King, S. (1991). Stable Isotope Studies of the Carbon, Nitrogen and Sulfur Cycles in the Black Sea and the Cariaco Trench. *Deep Sea Res. A. Oceanographic Res. Pap.* 38, S1003–S1019. doi:10.1016/S0198-0149(10)80021-4
- Gale, A. S., and Christensen, W. K. (1996). Occurrence of the Belemnite *Actinocamax Plenus* in the Cenomanian of SE France and its Significance. *bgsd* 43 (1), 68–77. doi:10.37570/bgsd-1996-43-08
- Gale, A. S., Jenkyns, H. C., Kennedy, W. J., and Corfield, R. M. (1993). Chemostratigraphy versus Biostratigraphy: Data from Around the Cenomanian-Turonian Boundary. *J. Geol. Soc.*, 150, 29–32. doi:10.1144/gsjgs.150.1.0029
- Gale, A. S., Jenkyns, H. C., Tsikos, H., van Breugel, Y., Sinninghe Damsté, J. S., Bottini, C., et al. (2019). High-resolution Bio- and Chemostratigraphy of an Expanded Record of Oceanic Anoxic Event 2 (Late Cenomanian-Early Turonian) at Clot Chevalier, Near Barrême, SE France (Vocontian Basin). *nos* 52 (1), 97–129. doi:10.1127/nos/2018/0445
- Goldberg, T., Poulton, S. W., Wagner, T., Kolonic, S. F., and Rehkämper, M. (2016). Molybdenum Drawdown during Cretaceous Oceanic Anoxic Event 2. *Earth Planet. Sci. Lett.* 440, 81–91. doi:10.1016/j.epsl.2016.02.006
- Hay, W. W. (2008). Evolving Ideas about the Cretaceous Climate and Ocean Circulation. *Cretaceous Res.* 29, 725–753. doi:10.1016/j.cretres.2008.05.025
- Herbin, J. P., Montadert, L., Müller, C., Gomez, R., Thurow, J., and Wiedmann, J. (1986). Organic-Rich Sedimentation at the Cenomanian-Turonian Boundary in Oceanic and Coastal Basins in the North Atlantic and Tethys North Atlantic Paleooceanography. *Spec. Publ. Geol. Soc.* 21, 389–422. doi:10.1144/GSL.SP.1986.021.01.28
- Hetzl, A., Böttcher, M. E., Wortmann, U. G., and Brumsack, H.-J. (2009). Paleo-Redox Conditions during OAE 2 Reflected in Demerara Rise Sediment Geochemistry (ODP Leg 207). *Palaeogeogr. Palaeoclimatol. Palaeoecol.* 273, 302–328. doi:10.1016/j.palaeo.2008.11.005
- Higgins, M. B., Robinson, R. S., Husson, J. M., Carter, S. J., and Pearson, A. (2012). Dominant Eukaryotic Export Production during Ocean Anoxic Events Reflects the Importance of Recycled NH<sub>4</sub><sup>+</sup>. *Proc. Natl. Acad. Sci.* 109, 2269–2274. doi:10.1073/pnas.1104313109
- Holmden, C., Jacobson, A. D., Sageman, B. B., and Hurtgen, M. T. (2016). Response of the Cr Isotope Proxy to Cretaceous Ocean Anoxic Event 2 in a Pelagic Carbonate Succession from the Western Interior Seaway. *Geochim. Cosmochim. Acta* 186, 277–295. doi:10.1016/j.gca.2016.04.039
- Huerta-Diaz, M. A., and Morse, J. W. (1992). Pyritization of Trace Metals in Anoxic Marine Sediments. *Geochim. Cosmochim. Acta* 56, 2681–2702. doi:10.1016/0016-7037(92)90353-K
- Jarvis, I., Lignum, J. S., Gröcke, D. R., Jenkyns, H. C., and Pearce, M. A. (2011). Black Shale Deposition, Atmospheric CO<sub>2</sub> drawdown, and Cooling during the

- Cenomanian-Turonian Oceanic Anoxic Event. *Paleoceanography* 26 (3), PA3201. doi:10.1029/2010pa002081
- Jefferies, R. P. S. (1962). The Paleoeology of the Actinocamax Plenus Subzone (Lowest Turonian) in the Anglo-Paris Basin. *Paleontology* 4 (4), 609–647.
- Jefferies, R. P. S. (1963). The Stratigraphy of the Actinocamax Plenus Subzone (Turonian) in the Anglo-Paris Basin. *Proc. Geologists' Assoc.* 74, 1–IN4. doi:10.1016/S0016-7878(63)80011-5
- Jenkyns, H. C., Gale, A. S., and Corfield, R. M. (1994). Carbon- and Oxygen-Isotope Stratigraphy of the English Chalk and Italian Scaglia and its Palaeoclimatic Significance. *Geol. Mag.* 131 (01), 1–34. doi:10.1017/s0016756800010451
- Jenkyns, H. C., Matthews, A., Tsikos, H., and Erel, Y. (2007). Nitrate Reduction, Sulfate Reduction, and Sedimentary Iron Isotope Evolution during the Cenomanian-Turonian Oceanic Anoxic Event. *Paleoceanography* 22, PA3208. doi:10.1029/2006PA001355
- Jenkyns, H. C., Dickson, A. J., Ruhl, M., and Boorn, S. H. J. M. (2017). Basalt-seawater Interaction, the Plenus Cold Event, Enhanced Weathering and Geochemical Change: Deconstructing Oceanic Anoxic Event 2 (Cenomanian-Turonian, Late Cretaceous). *Sedimentology* 64 (1), 16–43. doi:10.1111/sed.12305
- Jenkyns, H. C. (2010). Geochemistry of Oceanic Anoxic Events. *Geochem. Geophys. Geosyst.* 11 (3), Q03004. doi:10.1029/2009GC002788
- Jones, C. E., and Jenkyns, H. C. (2001). Seawater Strontium Isotopes, Oceanic Anoxic Events, and Seafloor Hydrothermal Activity in the Jurassic and Cretaceous. *Am. J. Sci.* 301, 112–149. doi:10.2475/ajs.301.2.112
- Jones, B., and Manning, D. A. C. (1994). Comparison of Geochemical Indexes Used for the Interpretation of Palaeoredox Conditions in Ancient Mudstones. *Chem. Geol.* 111 (1–4), 111–129. doi:10.1016/0009-2541(94)90085-X
- Junium, C. K., and Arthur, M. A. (2007). Nitrogen Cycling during the Cretaceous, Cenomanian-Turonian Oceanic Anoxic Event II. *Geochem. Geophys. Geosyst.* 8, 1–18. doi:10.1029/2006GC001328
- Keller, G., Adatte, T., Berner, Z., Chellai, E. H., and Stueben, D. (2008). Oceanic Events and Biotic Effects of the Cenomanian-Turonian Anoxic Event, Tarfaya Basin, Morocco. *Cretaceous Res.* 29 (5–6), 976–994. doi:10.1016/j.cretres.2008.05.020
- Krall, P., Slomp, C. P., Forster, A., and Kuypers, M. M. M. (2010). Phosphorus Cycling from the Margin to Abyssal Depths in the Proto-Atlantic during Oceanic Anoxic Event 2. *Palaeogeogr. Palaeodimatomol., Palaeoecol.* 295, 42–58. doi:10.1016/j.palaeo.2010.05.014
- Kuroda, J., Ogawa, N., Tanimizu, M., Coffin, M., Tokuyama, H., Kitazato, H., et al. (2007). Contemporaneous Massive Subaerial Volcanism and Late Cretaceous Oceanic Anoxic Event 2. *Earth Planet. Sci. Lett.* 256 (1–2), 211–223. doi:10.1016/j.epsl.2007.01.027
- Kuypers, M. M. M., Pancost, R. D., and Damsté, J. S. S. (1999). A Large and Abrupt Fall in Atmospheric CO<sub>2</sub> Concentration during Cretaceous Times. *Nature* 399, 342–345. doi:10.1038/20659
- Kuypers, M. M. M., Pancost, R. D., Nijenhuis, I. A., and Sinninghe Damsté, J. S. (2002). Enhanced Productivity Led to Increased Organic Carbon Burial in the Euxinic North Atlantic basin during the Late Cenomanian Oceanic Anoxic Event. *Paleoceanography* 17, 1–13. doi:10.1029/2000PA000569
- Kuypers, M. M. M., Lourens, L. J., Rijpstra, W. I. C., Pancost, R. D., Nijenhuis, I. A., and Sinninghe Damsté, J. S. (2004). Orbital Forcing of Organic Carbon Burial in the Proto-North Atlantic during Oceanic Anoxic Event 2. *Earth Planet. Sci. Lett.* 228, 465–482. doi:10.1130/G20458.110.1016/j.epsl.2004.09.037
- Lafargue, E., Marquis, F., and Pillot, D. (1998). Rock-Eval 6 Applications in Hydrocarbon Exploration, Production, and Soil Contamination Studies. *Rev. Inst. Fr. Pét.* 53, 421–437. doi:10.2516/ogst:1998036
- Lancelot, Y., Seibold, E., Ceppek, P., Dean, W. E., Eremeev, V., Gardner, J., et al. (1978). “Site 367: Cape Verde Basin,” in *Initial Reports of the Deep Sea Drilling Project*. 41, 163–232. doi:10.2973/dsdp.proc.41.103.1978
- McLennan, S. M. (2001). Relationships between the Trace Element Composition of Sedimentary Rocks and Upper continental Crust. *Geochem. Geophys. Geosyst.* 2. doi:10.1029/2000GC000109
- Mélières, F. (1978). “X-ray Mineralogy Studies, Leg 41, Deep Sea Drilling Project, Eastern North Atlantic Ocean,” in *Initial Reports of the Deep Sea Drilling Project*, 41. Editor Y. Lancelot (Washington: U. S. Government Printing Office), 1065–1086. doi:10.2973/dsdp.proc.41.142.1978
- Monteiro, F. M., Pancost, R. D., Ridgwell, A., and Donnadieu, Y. (2012). Nutrients as the Dominant Control on the Spread of Anoxia and Euxinia across the Cenomanian-Turonian Oceanic Anoxic Event (OAE2): Model-Data Comparison. *Paleoceanography* 27 (4), PA4209. doi:10.1029/2012pa002351
- Naafs, B. D. A., Monteiro, F. M., Pearson, A., Higgins, M. B., Pancost, R. D., and Ridgwell, A. (2019). Fundamentally Different Global marine Nitrogen Cycling in Response to Severe Ocean Deoxygenation. *Proc. Natl. Acad. Sci. USA* 116 (24), 24979–24984. doi:10.1073/pnas.1905553116
- O'Connor, L. K., Jenkyns, H. C., Robinson, S. A., Rimmelzwaal, S. R. C., Batenburg, S. J., Parkinson, I. J., et al. (2020). A Re-Evaluation of the Plenus Cold Event, and the Links between CO<sub>2</sub>, Temperature, and Seawater Chemistry during OAE 2. *Paleoceanogr. Paleoclimatol.* 35, e2019PA003631. doi:10.1029/2019PA003631
- Orth, C. J., Attrep, M., Quintana, L. R., Elder, W. P., Kauffman, E. G., Diner, R., et al. (1993). Elemental Abundance Anomalies in the Late Cenomanian Extinction Interval: A Search for the Source(s). *Earth Planet. Sci. Lett.* 117 (1–2), 189–204. doi:10.1016/0012-821x(93)90126-t
- Ostrander, C. M., Owens, J. D., and Nielsen, S. G. (2017). Constraining the Rate of Oceanic Deoxygenation Leading up to a Cretaceous Oceanic Anoxic Event (OAE-2: ~94 Ma). *Sci. Adv.* 3 (8), e1701020. doi:10.1126/sciadv.1701020
- Owens, J. D., Lyons, T. W., Li, X., Macleod, K. G., Gordon, G., Kuypers, M. M. M., et al. (2012). Iron Isotope and Trace Metal Records of Iron Cycling in the Proto-North Atlantic during the Cenomanian-Turonian Oceanic Anoxic Event (OAE-2). *Paleoceanography* 27, PA3223. doi:10.1029/2012PA002328
- Owens, J. D., Gill, B. C., Jenkyns, H. C., Bates, S. M., Severmann, S., Kuypers, M. M. M., et al. (2013). Sulfur Isotopes Track the Global Extent and Dynamics of Euxinia during Cretaceous Oceanic Anoxic Event 2. *Proc. Natl. Acad. Sci.* 110 (46), 18407–18412. doi:10.1073/pnas.1305304110
- Pancost, R. D., Crawford, N., Magness, S., Turner, A., Jenkyns, H. C., and Maxwell, J. R. (2004). Further Evidence for the Development of Photic-Zone Euxinic Conditions during Mesozoic Oceanic Anoxic Events. *J. Geol. Soc.* 161 (3), 353–364. doi:10.1144/0016764903-059
- Paul, C. R. C., Lamolda, M. A., Mitchell, S. F., Vaziri, M. R., Gorostidi, A., and Marshall, J. D. (1999). The Cenomanian-Turonian Boundary at Eastbourne (Sussex, UK): a Proposed European Reference Section. *Palaeogeogr. Palaeoclimatol. Palaeoecol.* 150 (1–2), 83–121. doi:10.1016/s0031-0182(99)00009-7
- Pearce, M. A., Jarvis, I., and Tocher, B. A. (2009). The Cenomanian-Turonian Boundary Event, OAE2 and Palaeoenvironmental Change in Epicontinental Seas: New Insights from the Dinocyst and Geochemical Records. *Palaeogeogr. Palaeoclimatol. Palaeoecol.* 280 (1–2), 207–234. doi:10.1016/j.palaeo.2009.06.01210.1016/j.palaeo.2009.06.012
- Pogge von Strandmann, P. A. E., Jenkyns, H. C., and Woodfine, R. G. (2013). Lithium Isotope Evidence for Enhanced Weathering during Oceanic Anoxic Event 2. *Nat. Geosci.* 6 (8), 668–672. doi:10.1038/ngeo1875
- Poulton, S. W., Henkel, S., März, C., Urquhart, H., Flögel, S., Kasten, S., et al. (2015). A continental-weathering Control on Orbitally Driven Redox-Nutrient Cycling during Cretaceous Oceanic Anoxic Event 2. *Geology* 43, 963–966. doi:10.1130/G36837.1
- Rau, G. H., Arthur, M. A., and Dean, W. E. (1987). 15N/14N Variations in Cretaceous Atlantic Sedimentary Sequences: Implication for Past Changes in marine Nitrogen Biogeochemistry. *Earth Planet. Sci. Lett.* 82 (3), 269–279. doi:10.1016/0012-821x(87)90201-9
- Redfield, A. C. (1958). The Biological Control of Chemical Factors in the Environment. *Am. Sci.* 46, 205–221.
- Ruvalcaba Baroni, I., van Helmond, N. A. G. M., Tsandev, I., Middelburg, J. J., and Slomp, C. P. (2015). The Nitrogen Isotope Composition of Sediments from the Proto-North Atlantic during Oceanic Anoxic Event 2. *Paleoceanography* 30, 923–937. doi:10.1002/2014PA002744.5
- Sageman, B. B., Meyers, S. R., and Arthur, M. A. (2006). Orbital Time Scale and New C-Isotope Record for Cenomanian-Turonian Boundary Stratotype. *Geol.* 34, 125–128. doi:10.1130/G22074.1
- Schlanger, S. O., and Jenkyns, H. C. (1976). Cretaceous Anoxic Events: Causes and Consequences. *Geol. Mijnb.* 55, 179–184.
- Schlanger, S. O., Arthur, M. A., Jenkyns, H. C., and Scholle, P. A. (1987). The Cenomanian-Turonian Oceanic Anoxic Event, I. Stratigraphy and Distribution of Organic Carbon-Rich Beds and the marine  $\delta^{13}\text{C}$  Excursion. *Geol. Soc. Lond. Spec. Publications* 26 (1), 371–399. doi:10.1144/gsl.sp.1987.026.01.24
- Scholle, P. A., and Arthur, M. A. (1980). Carbon Isotope Fluctuations in Cretaceous Pelagic Limestones: Potential Stratigraphic and Petroleum Exploration Tool.



- Am. Assoc. Pet. Geol. Bull.* 60 (1), 67–87. doi:10.1306/2f91892d-16ce-11d7-8645000102c1865d
- Schouten, S., Hopmans, E. C., Forster, A., van Breugel, Y., Kuypers, M. M. M., and Sinninghe Damsté, J. S. (2003). Extremely High Sea-Surface Temperatures at Low Latitudes during the Middle Cretaceous as Revealed by Archaeal Membrane Lipids. *Geol.* 31, 1069–1072. doi:10.1130/G19876.1
- Sigman, D. M., Karsh, K. L., and Casciotti, K. L. (2009). “Nitrogen Isotopes in the Ocean,” in *Encyclopedia of Ocean Sciences*. Editors J.H. Steele, S.A. Thorpe, and K.K. Turekian (Oxford: Academic Press), 40–54. doi:10.1016/b978-012374473-9.00632-9
- Sinninghe Damsté, J. S., and Köster, J. (1998). A Euxinic Southern North Atlantic Ocean during the Cenomanian/Turonian Oceanic Anoxic Event. *Earth Planet. Sci. Lett.* 158, 165–173. doi:10.1016/S0012-821X(98)00052-1
- Sinninghe Damsté, J. S. S., Kuypers, M. M. M., Pancost, R. D., and Schouten, S. (2008). The Carbon Isotopic Response of Algae, (Cyano)bacteria, Archaea and Higher Plants to the Late Cenomanian Perturbation of the Global Carbon Cycle: Insights from Biomarkers in Black Shales from the Cape Verde Basin (DSDP Site 367). *Org. Geochem.* 39, 1703–1718. doi:10.1016/j.orggeochem.2008.01.012
- Sinninghe Damsté, J. S., van Bentum, E. C., Reichart, G.-J., Pross, J., and Schouten, S. (2010). A CO<sub>2</sub> Decrease-Driven Cooling and Increased Latitudinal Temperature Gradient during the Mid-cretaceous Oceanic Anoxic Event 2. *Earth Planet. Sci. Lett.* 293 (1–2), 97–103. doi:10.1016/j.epsl.2010.02.027
- Sinton, C. W., and Duncan, R. A. (1997). Potential Links between Ocean Plateau Volcanism and Global Ocean Anoxia at the Cenomanian-Turonian Boundary. *Econ. Geol.* 92, 836–842. doi:10.2113/gsecongeo.92.7-8.836
- Snow, L. J., Duncan, R. A., and Bralower, T. J. (2005). Trace Element Abundances in the Rock Canyon Anticline, Pueblo, Colorado, marine Sedimentary Section and Their Relationship to Caribbean Plateau Construction and Oxygen Anoxic Event 2. *Paleoceanography* 20 (3), PA3005. doi:10.1029/2004pa00109310.1029/2005pa001222
- Stüeken, E. E., Kipp, M. A., Koehler, M. C., and Buick, R. (2016). The Evolution of Earth’s Biogeochemical Nitrogen Cycle. *Earth-Science Rev.* 160, 220–239. doi:10.1016/j.earscirev.2016.07.007
- Summons, R. E., Jahnke, L. L., Hope, J. M., and Logan, G. A. (1999). 2-Methylhopanoids as Biomarkers for Cyanobacterial Oxygenic Photosynthesis. *Nature* 400, 554–557. doi:10.1038/23005
- Takashima, R., Nishi, H., Hayashi, K., Okada, H., Kawahata, H., Yamanaka, T., et al. (2009). Litho-, Bio- and Chemostratigraphy across the Cenomanian/Turonian Boundary (OAE 2) in the Vocontian Basin of southeastern France. *Palaeogeogr. Palaeoclimatol. Palaeoecol.* 273, 61–74. doi:10.1016/j.paleo.2008.12.00110.1016/j.paleo.2008.12.001
- Thomazo, C., and Papineau, D. (2013). Biogeochemical Cycling of Nitrogen on the Early Earth. *Elements* 9, 345–351. doi:10.2113/gselements.9.5.345
- Thunell, R. C., Sigman, D. M., Muller-Karger, F., Astor, Y., and Varela, R. (2004). Nitrogen Isotope Dynamics of the Cariaco Basin, Venezuela. *Glob. Biogeochem. Cycles* 18 (3), GB3001. doi:10.1029/2003GB002185
- Topper, R. P. M., Trabucho Alexandre, J., Tuenter, E., and Meijer, P. T. (2011). A Regional Ocean Circulation Model for the Mid-cretaceous North Atlantic Basin: Implications for Black Shale Formation. *Clim. Past* 7, 277–297. doi:10.5194/cp-7-277-2011
- Trabucho Alexandre, J., Tuenter, E., Henstra, G. A., van der Zwan, K. J., van de Wal, R. S. W., Dijkstra, H. A., et al. (2010). The Mid-cretaceous North Atlantic Nutrient Trap: Black Shales and OAEs. *Paleoceanography* 25, PA4201. doi:10.1029/2010PA001925
- Tribouillard, N., Algeo, T. J., Lyons, T., and Riboulleau, A. (2006). Trace Metals as Paleoredox and Paleoproductivity Proxies: An Update. *Chem. Geology* 232, 12–32. doi:10.1016/j.chemgeo.2006.02.012
- Tribouillard, N., Algeo, T. J., Baudin, F., and Riboulleau, A. (2012). Analysis of marine Environmental Conditions Based Onmolybdenum-Uranium Covariation-Applications to Mesozoic Paleocyanography. *Chem. Geology* 324–325, 46–58. doi:10.1016/j.chemgeo.2011.09.009
- Tsikos, H., Jenkyns, H. C., Walsworth-Bell, B., Petrizzo, M. R., Forster, A., Kolonic, S., et al. (2004). Carbon-isotope Stratigraphy Recorded by the Cenomanian-Turonian Oceanic Anoxic Event: Correlation and Implications Based on Three Key Localities. *J. Geol. Soc.* 161 (4), 711–719. doi:10.1144/0016-764903-077
- Tucholke, B. E., Sibuet, J.-C., Klaus, A., Arnaoldi, M., Delius, H., Engström, A. V., et al. (2004). “Site 1276,”. *Proc. ODP, Init. Repts.* Editors B.E. Tucholke, J.-C. Sibuet, and A. Klaus (College Station, TX: Ocean Drilling Program), 210, 1–358. doi:10.2973/odp.proc.ir.210.103.2004
- Turgeon, S. C., and Creaser, R. A. (2008). Cretaceous Oceanic Anoxic Event 2 Triggered by a Massive Magmatic Episode. *Nature* 454 (7202), 323–326. doi:10.1038/nature07076
- Tyrrell, T. (1999). The Relative Influences of Nitrogen and Phosphorus on Oceanic Primary Production. *Nature* 400, 525–531. doi:10.1038/22941
- van Bentum, E. C., Reichart, G.-J., Forster, A., and Sinninghe Damsté, J. S. (2012). Latitudinal Differences in the Amplitude of the OAE-2 Carbon Isotopic Excursion: pCO<sub>2</sub> and Paleo Productivity. *Biogeosciences* 9 (2), 717–731. doi:10.5194/bg-9-717-2012
- Van Capellen, P., and Ingall, E. D. (1994). Benthic Phosphorus Regeneration, Net Primary Production, and Ocean Anoxia: a Model of the Coupled marine Biogeochemical Cycles of Carbon and Phosphorus. *Paleoceanography* 9, 677–692. doi:10.1029/94PA01455
- van Helmond, N. A. G. M., Ruvalcaba Baroni, I., Sluijs, A., Sinninghe Damsté, J. S., and Slomp, C. P. (2014a). Spatial Extent and Degree of Oxygen Depletion in the Deep Proto-North Atlantic basin during Oceanic Anoxic Event 2. *Geochem. Geophys. Geosyst.* 15 (11), 4254–4266. doi:10.1002/2014GC005528
- van Helmond, N. A. G. M., Sluijs, A., Reichart, G.-J., Sinninghe Damsté, J. S., Slomp, C. P., and Brinkhuis, H. (2014b). A Perturbed Hydrological Cycle during Oceanic Anoxic Event 2. *Geology* 42, 123–126. doi:10.1130/G34929.1
- van Hinte, J. E., Wise, S. W., Jr, Biart, B. N. M., Covington, J. M., Dunn, D. A., Haggerty, J. A., et al. (1993). “Site 603,”. *Proc. DSDP, Init. Repts.* Editors J. E. van Hinte and S. W. Wise Jr. (College Station, TX: Ocean Drilling Program), 93, 25–276. doi:10.2973/dsdp.proc.93.102.1987
- Wedepohl, K. H. (1971). “Environmental Influences on the Chemical Composition of Shales and Clays,” in *Physics and Chemistry of the Earth*. Editors L.H. Ahrens, F. Press, S.K. Runcorn, and H.C. Urey (Oxford: Pergamon), 305–333.
- Westermann, S., Vance, D., Cameron, V., Archer, C., and Robinson, S. A. (2014). Heterogeneous Oxygenation States in the Atlantic and Tethys Oceans during Oceanic Anoxic Event 2. *Earth Planet. Sci. Lett.* 404, 178–189. doi:10.1016/j.epsl.2014.07.018
- Zhang, X., Sigman, D. M., Morel, F. M. M., and Kraepiel, A. M. L. (2014). Nitrogen Isotope Fractionation by Alternative Nitrogenases and Past Ocean Anoxia. *Proc. Natl. Acad. Sci. USA* 111, 4782–4787. doi:10.1073/pnas.1402976111
- Zheng, X.-Y., Jenkyns, H. C., Gale, A. S., Ward, D. J., and Henderson, G. M. (2013). Changing Ocean Circulation and Hydrothermal Inputs during Ocean Anoxic Event 2 (Cenomanian-Turonian): Evidence from Nd-Isotopes in the European Shelf Sea. *Earth Planet. Sci. Lett.* 375, 338–348. doi:10.1016/j.epsl.2013.05.053

**Conflict of Interest:** The authors declare that the research was conducted in the absence of any commercial or financial relationships that could be construed as a potential conflict of interest.

**Publisher’s Note:** All claims expressed in this article are solely those of the authors and do not necessarily represent those of their affiliated organizations, or those of the publisher, the editors and the reviewers. Any product that may be evaluated in this article, or claim that may be made by its manufacturer, is not guaranteed or endorsed by the publisher.

Copyright © 2021 Riquier, Cadeau, Danzelle, Baudin, Pucéat and Thomazo. This is an open-access article distributed under the terms of the Creative Commons Attribution License (CC BY). The use, distribution or reproduction in other forums is permitted, provided the original author(s) and the copyright owner(s) are credited and that the original publication in this journal is cited, in accordance with accepted academic practice. No use, distribution or reproduction is permitted which does not comply with these terms.